# Geosynthetics in basecourse stabilisation December 2015

SA Bagshaw, PR Herrington, P Kathirgamanathan and SR Cook
Opus International Consultants Ltd

**NZ Transport Agency research report 574 – 2nd edition**
Contracted research organisation – Opus International Consultants Ltd

ISBN 978-0-478-44577-0 (electronic)
ISSN 1173-3764 (electronic)

NZ Transport Agency
Private Bag 6995, Wellington 6141, New Zealand
Telephone 64 4 894 5400; facsimile 64 4 894 6100
research@nzta.govt.nz
www.nzta.govt.nz

Bagshaw, SA, PR Herrington, P Kathirgamanathan and SR Cook (2015) Geosynthetics in basecourse stabilisation. *NZ Transport Agency research report 574.* 64pp.

Opus International Consultants Ltd was contracted by the NZ Transport Agency in 2013 to carry out this research.



**Keywords:** basecourse, discrete element, finite element (FE), geocell, geogrid, geosynthetic, gravel, pavement, repeated load tri-axial (RLT), stabilisation

# An important note for the reader

The NZ Transport Agency is a Crown entity established under the Land Transport Management Act 2003. The objective of the Agency is to undertake its functions in a way that contributes to an efficient, effective and safe land transport system in the public interest. Each year, the NZ Transport Agency funds innovative and relevant research that contributes to this objective.

The views expressed in research reports are the outcomes of the independent research, and should not be regarded as being the opinion or responsibility of the NZ Transport Agency. The material contained in the reports should not be construed in any way as policy adopted by the NZ Transport Agency or indeed any agency of the NZ Government. The reports may, however, be used by NZ Government agencies as a reference in the development of policy.

While research reports are believed to be correct at the time of their preparation, the NZ Transport Agency and agents involved in their preparation and publication do not accept any liability for use of the research. People using the research, whether directly or indirectly, should apply and rely on their own skill and judgement. They should not rely on the contents of the research reports in isolation from other sources of advice and information. If necessary, they should seek appropriate legal or other expert advice.

# Errata

This report was originally published in September 2015.

The report has been significantly revised by the authors, with changes to the text and graphics to correct inaccuracies in the original report.

This second edition of the report, published in December 2015, supersedes the previous edition.

# Acknowledgements

The authors would like to thank:

Sharon Hunter-Smith (Geofabrics NZ), Graeme Bell (GeoTech Systems), David Hutchison (Downer), and Deven Singh (Wellington City Council) for their participation in the project steering group. Martin Gribble (NZ Transport Agency) and Bryan Pidwerbesky (Fulton Hogan Ltd) for peer review of the final report. Geofabrics NZ, Geofabrics Australia and GeoTech Systems Ltd NZ for supply of geogrids and geocell samples to the project. Road Science Ltd for supply of bitumen emulsion for preparing chipseals and NZ Transport Agency/CAPTIF for supplying the aggregate and initial materials analysis data. Mark Wayne (Tensar International) for RLT testing and analysis of the aggregate materials supplied and for useful discussions and information.

# Abbreviations and acronyms

| | |
|---|---|
| AASHTO | American Association of State Highway and Transportation Officials |
| ALF | Austroads Accelerated Loading Facility |
| Austroads | Association of Australasian Road Transport and Traffic Agencies |
| BCR | basecourse reduction |
| CAPTIF | Canterbury Accelerated Pavement Testing Facility |
| CBR | California bearing ratio |
| CIRCLY | international pavement design software |
| DD | dry density |
| DOT | Department of Transport |
| ESL | equivalent standard axle-loads |
| FE | finite element |
| FEM | finite element modelling |
| GMA | Geosynthetic Materials Association |
| kN | kilo Newtons |
| MIF | modulus improvement factor |
| NDM | nuclear density meter |
| ORAPT | Opus Research Accelerated Pavement Tester |
| Pen grade | penetration grade |
| PUMA | precision unbound material analyser |
| RLT | repeated load tri-axial test |
| TBR | traffic benefit ratio |
| Transport Agency | New Zealand Transport Agency |
| WD | wet density |
| % Comp | percent compaction |
| % M | percent moisture |

# Contents

# Executive summary

This report presents the results of exploratory investigations to assess the potential benefits of including geogrid materials in basecourse pavements prepared using Canterbury River Run gravel aggregates. Originally designated M/5, we have used the more generic name of River Run gravel. The Opus Research Accelerated Pavement Tester (ORAPT) does not represent a field trial, but acts as a comparative tool, applying loads that mimic those applied in the field, in between that of a lightweight wheel tracker and a full-sized facility, such as the Canterbury Accelerated Pavement Testing Facility (CAPTIF) or the Austroads Accelerated Loading Facility (ALF).

Stabilisation of unbound granular pavements with the aim of increasing their life, reducing material usage and permitting the use of marginal materials is topical as optimal aggregates become ever more difficult and expensive to source and transport. A low-cost aggregate material is readily available for use in Canterbury New Zealand, but it is thought that the round particle shapes may cause suboptimal particle packing and interaction characteristics that will lead it to shear readily. The use of geosynthetics (in this case geogrids) to stabilise the aggregate against shear strain and consolidation was proposed. In particular, the research investigated whether geogrids might:

- be able to stabilise basecourses prepared from the River Run aggregates against shear
- reduce the rate of rutting of basecourses prepared from the aggregate.

Originally the project title was ‘Geosynthetics in basecourse reinforcement’. However, the concept of strengthening, stiffening or reinforcing pavement basecourse with geogrids is now being superseded internationally by the concept of stabilisation. While the practical outcomes may be the same, it is argued that neither the concepts nor the theoretical treatments are equivalent, therefore the title of this report has been modified to reflect this.

## Rutting rates of unstabilised basecourse

The rate of rutting of basecourses prepared using the River Run aggregate with no stabilisation was very high. Rut depths of approximately 100mm formed after around 10,000 passes of the Austroads standard tyre at 20kN load. The rutting rate did not improve appreciably after a single coat 3/5 racked-in chipseal was applied. However, the rutting rate decreased dramatically when a 20mm thick cold-mix asphalt layer was applied. The application of the asphalt highlighted the ability of the River Run basecourse to support loads and to resist shearing when the surface of the basecourse was confined.

## Rutting rates of geogrid-stabilised basecourse

Two different geogrids were trialled in the basecourse,with chipseal surfacing. One of the geogrids was trialled at three different positions: at the sub-base/basecourse interface, at basecourse half-height and at basecourse ¾ height. The other geogrid was trialled only at the sub-base/basecourse interface. The final rut depth for the samples with a large-aperture tri-axial grid (approx 60mm aperture size) placed either at the base or at half-height was reduced by approximately 40% over that of the unstabilised basecourse. The sample with geogrid at ¾ height showed no reduction in rutting rate over that of the unstabilised sample. The second, a smaller aperture square-type geogrid (approximately 40mm aperture size), placed at the sample base, provided an approximately 60% reduction in final rut depth over the unstabilised sample. These results highlight that:

- geogrid can provide substantial stabilisation against shear of the River Run aggregate when installed at the base or at mid-height of the basecourse

- placing geogrid closer to the top surface appears to provide less stabilisation
- close attention to size matching of grid and aggregate is very important.

## Conclusions and recommendations

The results of this mid-scale laboratory study demonstrate the potential for geogrids to stabilise River Run gravel aggregate against shear/rutting, as long as the surface of the basecourse is confined with a binder or a resilient surfacing such as asphalt. The lack of particle interlock makes the River Run aggregate highly mobile and if the surface is not confined it will shear under the wheel load. However, if the surface of the basecourse is confined, and the bulk of the basecourse is further stabilised, then it appears the aggregate skeleton along with the grading are sufficient to provide some degree of pavement strength and stability. This aspect of the findings should be explored further with different binders in the surface and with binders and geosynthetic stabilisation combined. Analysis of the stress and strain relationships within the basecourse as affected by geosynthetics via the use of embedded sensors might also be investigated.

The conditions used in this investigation were laboratory conditions and may not closely represent those found in the field. Time, budget and additional unforeseen samples meant that repeat samples were not able to be completed within the scope of the project. This is quite problematic, so repetition of selected samples to establish the repeatability of the experiment should be investigated. Longer-term and field studies are also needed to examine the behaviour of the River Run aggregate basecourse under service conditions. Time did not permit the testing of geocell stabilisation, but this should be investigated. The addition of a binder (cement or bitumen) throughout the basecourse rather than just the surface region, might also be investigated. Overall, the recommendation from this work is that geogrid placement at the basecourse/sub-base interface in partnership with a resilient asphalt surfacing may produce a stable River Run-based basecourse, at least for low-volume, low-performance roads. It should also be noted that the size of the tri-axial geogrid used may in fact have been inappropriate and that a different sized tri-axial geogrid may perform differently with this aggregate basecourse. It should also be noted, that compaction in multiple lifts may also improve overall performance. Further trials are necessary to verify these issues.

# Abstract

The application of geosynthetics (ie geogrids) for the stabilisation of basecourses prepared with a River Run rounded gravel aggregate was investigated. Reductions in the rate of rut formation by up to 60% were observed when geogrids were included either at the basecourse/sub-base interface or at half-height of the basecourse. It was found that the basecourse rutted rapidly if the surface was not confined, due to the lack of particle interlock and surface confining stress. If the surface was confined with a thin (ie <40mm) asphalt layer to bind together the particles in the surface, then the aggregate provided significant support with significantly reduced rutting even without the addition of geosynthetic stabilisation. Additional investigation is needed to determine the stress/strain relationships, lifetimes and loads that may be expected to be obtained and supported with different combinations of surface binding and geogrid basecourse stabilisation.

# 1 Introduction

The purpose of this research project was to examine the possible pavement performance enhancements (lifetime, maintenance, materials use) that might be derived through the installation of geosynthetics, in the form of geogrids, in the pavement basecourse. The main aim of the project was to determine if it is possible to improve pavement performance (shear resistance) of a particular aggregate that may otherwise be considered to be compromised in terms of its physical structure or geology. In particular therefore, the project examined the geogrid stabilisation of a specific rounded aggregate, which under normal conditions exhibits low shear resistance. This project focused on the development of resilience, over and above that which is autogenously derived in basecourse through compaction, via the introduction of geogrids into a basecourse prepared from a specific Canterbury gravel aggregate. Geotextiles, which have been the subject of a previous Transit New Zealand study (Hudson and East 1991) and are generally designed to perform different tasks such as filtering but are also used in conjunction with geogrids, were not considered in this project. It should also be recognised that the concept of ‘reinforcement’, which implies strength addition, is being replaced by more recent concepts describing ‘stabilisation’, which rather implies strength retention through locking particles into place.

A literature review examines the area of geosynthetic (geogrid and geocell) stabilisation reported to date that has informed the understanding of the design, manufacture, application and mechanisms of action of geogrids and geocells and pavement design methods. The experimental section describes the testing methods and sample designs that were adopted, and then presents the experimental results. In different literature cases the samples or road trials were surfaced with asphalt or with chipseals or with no particular surfacing. Given that the focus here is on the performance of the geosynthetic in the sample, the surfacing is not considered further in the discussion. The conclusions reached therefore, attempt to provide insight into the general outcomes, and tentative recommendations are offered for application of the technologies with regard to the aggregate studied.

# 2 Literature review

## 2.1 Geosynthetic basecourse stabilisation

A large proportion of the New Zealand highway network is constructed from unbound flexible pavements with thin asphalt or chipseal coatings (Transit NZ et al 2005). Very highly trafficked sections or sections of high stress, such as motorways, are asphalt coated, which offers higher strength than chipseals, but at higher cost. The strength of some pavement sections is augmented through the addition of binders (bitumen or cement) into the pavement (basecourse) layers. The strength, as represented by the stiffness, and resistance to deformation of the flexible pavement, is developed through compaction and subsequent three-dimensional interlocking and friction between the individual aggregate particles in the four different layers of the pavement (subgrade, sub-base, basecourse, surface layer) (Jones and Dawson 1989). It has been identified that not only are the integrities of the sub-base and the basecourse paramount to the formation of a resilient pavement, but also that resilience in both the upper-most surface layer and underlying subgrade must work in concert with the rest of the pavement. Failure in any of the four sections of the pavement can therefore result in failure of the whole, either by materials degradation, mass flow, or water induced erosion. The four factors identified as the most important to be considered regarding basecourse resilience are in order: aggregate type, aggregate grading, moisture content and tyre contact pressure (ie load). The aggregate type, grading and moisture content can be controlled during design and construction. The inter-particular friction and particle interlock generated during construction and compaction can be modified by the addition of outside factors, such as geosynthetics, into the design.

Typically the basecourse is formed by compaction of a matrix of individual aggregate particles of an envelope of sizes, and is subsequently treated as a continuous matrix system. We know, however, that inter-particular friction and interlock at the local level form the fundamental building blocks of the basecourse matrix. In three dimensions therefore, the confining stresses of any individual building block unit are developed within the wider matrix by compaction of the aggregate building blocks against one another. Geogrids/cells are, in the main part, applied to augment these phenomena through stabilisation of the sub-base/basecourse interface via mechanically induced particle interlock and friction.

Particle packing (Yedeti et al 2013) and shakedown theories (Song and Ooi 2010) both suggest that under certain load stress (which will differ depending on the details of the individual pavement) the pavement will accumulate a degree of permanent deformation under that load, which will manifest as a rut. Depending on the design and construction of the pavement, the environment and the applied loads, this rut will remain small, or it will increase in size, leading to eventual failure of the pavement. Other failures can also occur due to aggregate breakdown, movement of aggregate particles within the pavement layer (shear/mass flow) and water ingress which can wash certain fractions of the aggregate out of the pavement, lowering the density and causing failure.

Particle packing theories inform us that certain packing density maxima are possible for any given particle (aggregate) grading envelope, but also that these theoretical packing densities, on the whole, cannot be achieved with mass mixing and compacting techniques. Indeed, particle packing theories suggest that maximal packing densities, regardless of the laying and compaction technologies, cannot be achieved with dense-graded envelopes, rather that certain gap grading needs to be considered in order to achieve maximal packing densities (Yedeti et al 2013; Abdel-Jawad and Abdullah 2002; Shen and Yu 2011). This consideration is important from the viewpoint of pavement strength in that the higher the packing density the greater the inter-particle interactions (friction and interlock) leading to increased strength. While alternatives such as the new gap graded *Hi-Lab* system (van Blerk and Fahey 2013) are being investigated in New Zealand, in the absence of alternatives, the current NZTA M/4 dense-graded aggregate envelope is

widely specified for highway construction. Where local materials, processing or cost constraints mean that the M/4 aggregate standard is difficult to obtain, we should seek other methods that will assist designers and contractors to reach the M/4 standard and subsequently to restrict the rate and/or amount of pavement permanent deformation. In the absence of achieving theoretical maximal densities, or in the absence of M/4 specified aggregate at reasonable cost, the addition of mechanical stabilisation via geosynthetics may achieve these aims.

Funding for road construction and maintenance is becoming ever more constrained; the price of bitumen is continuing to climb and the availability and cost of quality aggregates are becoming ever more difficult. There is therefore, a drive to use less material (aggregate and bitumen), cheaper (eg more marginal) materials and more local materials, while at the same time minimising premature failure through smarter design. At the heart of pavement designing with geosynthetics are the two concepts of traffic benefit ratio (TBR), ie the number of equivalent standard axle-load (ESL) passes that a pavement of the same thickness will accept; and basecourse reduction (BCR), ie the amount that the thickness of a pavement can be reduced, for the same number of ESL passes. These concepts both aim to reduce construction and maintenance costs either in lifetime extension and/or materials use, respectively (Perkins 2001). While reductions in pavement permanent deformation can be achieved with sub-base and/or basecourse stabilisation with cement (Lay 1990a), bitumen (Lay 1990b) or lime (Weston and Edwards 2004) (or combinations thereof), the installation of geosynthetic materials (geotextiles, geogrids, geocells) into pavement structures has now become commonplace. Significant research has now been undertaken both by industry and academic laboratories to understand how these different geosynthetics work, how to model their actions and how to optimise their design and installation in pavements (Berg et al 2000).

## 2.2 Geogrids

Geogrids have been introduced from soil stabilisation applications into pavement reinforcement applications, with the industry touting significant success especially in applications where the subgrade and/or sub-base have low stiffness or low bearing capacity. Geogrids are widely use for the stabilisation of soils and rocks in walls, banks and other landforms, and their use is increasing year on year for pavement stabilisation in New Zealand. Geogrids are considered to be two-dimensional civil engineering materials, most commonly prepared from sheets of high tensile strength, high-density polyethylene and polypropylene (figures 2.1, 2.2) or from strips of high-strength polymers bonded together (polyamide, polyester) (figure 2.3). The majority are now prepared with a punch and draw technique, but some manufacturers prefer to use adhesive or laser bonding systems. Geogrids have unique sized apertures, of differing shapes and sizes, depending on the manufacturer or the application. The most common is the uni-dimensional geogrid (figure 2.1) with long slit-like apertures which is used in retaining wall/earthen wall applications, but not in pavements.

**Figure 2.1 Uni- dimensional geogrid**

Uniaxial Geogrid

The two-dimensional geogrids with square apertures (figures 2.2 and 2.3) have been the mainstays for earthen wall, embankment and pavement reinforcement over the past 10–20 years.

**Figure 2.2 Two- dimensional geogrid (punch and draw)**

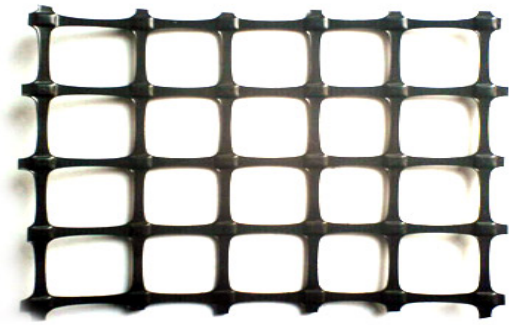

**Figure 2.3 Laser bonded strip geogrid**

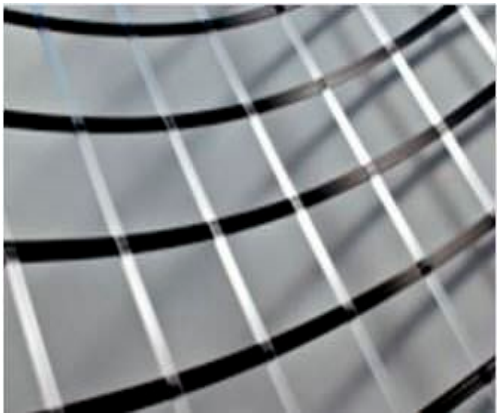

However, bi-axial geogrids are being superseded by new tri-axial and hexagonal geogrid designs (figures 2.4 and 2.5) by some manufacturers. These shapes are proposed to provide lines of force in all different (horizontal) directions simultaneously, thereby resisting the formation of specific lines of force that can arise with the square grids (www.tensarcorp.com). However, while there remains considerable debate in the industry, it has been suggested that depending on the specific properties of the product, these force lines can be better distributed with the new tri-axial materials.

**Figure 2.4 Hexagonal, polymer geogrid**

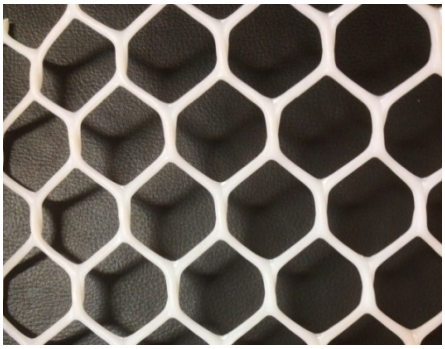

**Figure 2.5 Tri- axial geogrid**

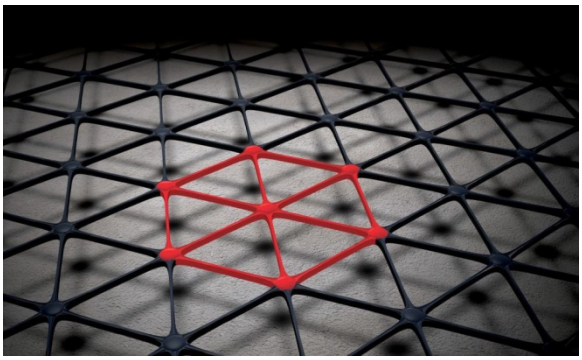

The earliest investigations of geotextiles in pavements were reported in the UK around 1981/82 (Potter and Currer 1981; Ruddock et al 1982; Ruddock 1982) and the first major analyses of the use of geogrids were reported slightly later (Netlon Industries 1984; Chaddock 1988). Since those early reports, work has focused almost exclusively on sub-base 'stabilisation' and the basecourse 'reinforcement' that results from this. This stabilisation occurs when geogrids are placed at the interface of the basecourse and the sub-base of the flexible pavement. This has been demonstrated to improve consistently the service life of a pavement and/or to provide equivalent performance with reduced structural section (BCR) (Perkins 2001). There remains some debate as to the ability of the designer to simultaneously design in both TBR and BCR with some suggesting it is possible, but the majority considering that when a designer decides to design in one of the two improvements, the other effect may also occur (Perkins et al 2009).

In a major review of the effectiveness of geosynthetics in road base reinforcement for the Geosynthetic Materials Association (GMA) several trends were identified (Berg et al 2000):

- TBR was identified as a common measure of reinforcement performance (geogrids providing TBR between 1.5 and 70).
- Basecourse reduction was cited as the major reason for reinforcement (BCR up to 50% is possible).
- There was little uniformity between tests employed, so any conclusions could only be general.
- No generally accepted properties, property values, indices or performances for different geogrids were available.

But the review did identify the important component actions that provide the reinforcement by:

- prevention of lateral particle spread (stabilisation rather than reinforcement)
- increased confinement and thus increased elastic modulus of layers
- improved vertical stress distribution through retention of skeleton position in space
- reduced shear stress within the stabilised layers.

The importance of the 'shear interaction' between the 'relatively stiff' geosynthetic and the aggregate to achieve the necessary components of stabilisation was emphasised. These are, however, qualitative statements with some progress having been made to develop methods for quantifying these characteristics, and further effort is being expended in this area. The experimental methods were based around modifications of confinement models in a small-scale laboratory, small-scale field studies and shear or pull-out tests. Pull-out tests have been used extensively to determine the engineering properties of the geogrid materials themselves in addition to the mechanisms of their action.

The findings of comparative tests at the time indicated:

1 There appeared to be no meaningful correlation between geogrid confinement and aperture size, percent open area, ultimate junction strength, ultimate wide width tensile strength/stiffness, or interface friction.

2 There did appear to be significant correlation between geosynthetic confinement and:

   a initial junction stiffness

   b initial pull-out force

   c initial wide-width tensile strength/stiffness.

3 Basecourse stabilisation appeared to be more effective with coarser gradations over finer, but stabilisation effectiveness with fine materials such as sand, could also be significant.

4 Basecourse stabilisation by geogrids was more effective over low bearing strength subgrades than high (ie the effects can actually be seen). As the California bearing ratio (CBR), or more generally the bearing capacity, approached a value of 8 (ie a stiff, high capacity material), then the benefits of additional geogrid stabilisation were shown to decrease.

5 Basecourse stabilisation was more effective with thinner basecourses. Basecourses with added geogrids showed decreasing benefits with increasing thickness beyond approximately 250mm, which was probably due to the inherent strength of thicker pavement layers and their ability to better disperse loads.

Finding 1 (above) would initially seem to be at odds with the logical argument regarding the implementation of geogrids insofar as there must be a relationship between the size of the grid aperture and the size of the aggregate that can be effectively constrained within the apertures of that grid. However, it has been shown in many studies that geogrids with apertures around 30mm can effectively constrain sandy materials, thereby supporting the assertion. It was suggested though, that there is a maximum particle size for a given aperture size that will be effectively constrained (ie aggregate particles do actually need to fit into the apertures to some degree).

Finding 2 (above) would suggest there are several energy barriers that must be overcome before any significant changes (permanent deformation) to the aggregate assembly or structure will occur. Installation of a geogrid into the pavement increases the magnitudes of these energy barriers via physical confinement mechanisms (ie stabilisation of the positions of particles).

Finding 3 (above) is linked to Finding 1, but while it is so that some degree of particle/aperture size matching might be necessary, it has been shown that large aperture geogrids can effectively reinforce sand structures thereby implying that the particle confinement effect can act over significant distance.

Findings 4 and 5 (above) demonstrate that while the stabilisation can act over significant distance, there are limits beyond which no additional performance benefits will be accrued by including geosynthetics into a pavement structure.

Other than the large GMA study (Berg et al 2000), other reviews, experimental and numerical investigations have been published attempting to understand the geogrid reinforcement/stabilisation effects and mechanisms. A large amount of this work occurred in the late 1990s and early 2000s and has been summarised (Perkins 2001; Koerner 1998; Perkins and Ismeik 1997). There does not appear to have been a comprehensive review of work undertaken post 2001.

It is argued that ‘Lateral restraint or lateral confinement’ of the aggregate and hence the basecourse matrix, may be misleading terms. The lateral restraint actually develops through interfacial friction between the aperture ribs of the geosynthetic and the aggregate particles and is possibly better considered to be a ‘shear-resisting interface’ which philosophically describes stabilisation (Perkins 1999). When a vertical load (from traffic) is applied to a pavement the aggregate will act to move laterally, away from that load, unless it is restrained in some way, such as by a confining stress (the horizontal mass of the pavement itself), a mechano-chemical means (cement, bitumen, lime) or a mechanical means (geogrid). In the case of mechanical confinement with geogrids, interaction between the aggregate and the geogrid allows the shearing load to be transferred from the particles of the pavement layer into a tensile load of the geogrid, which thereby effectively distributes that load over a larger area (figure 2.6). It was also suggested in that work that this tensile strain does not exist until traffic loads are actually applied to the pavement, meaning therefore that a certain (small) amount of deformation could occur until the tensile strain is established. While this might be debatable, in that it can be argued the construction of the pavement with the geogrid established a tensile strain, this small amount of initial plastic deformation might be equated to ‘shakedown’.

**Figure 2.6 Lateral transfer and spread of load on unbound pavement by geogrid reinforcement**

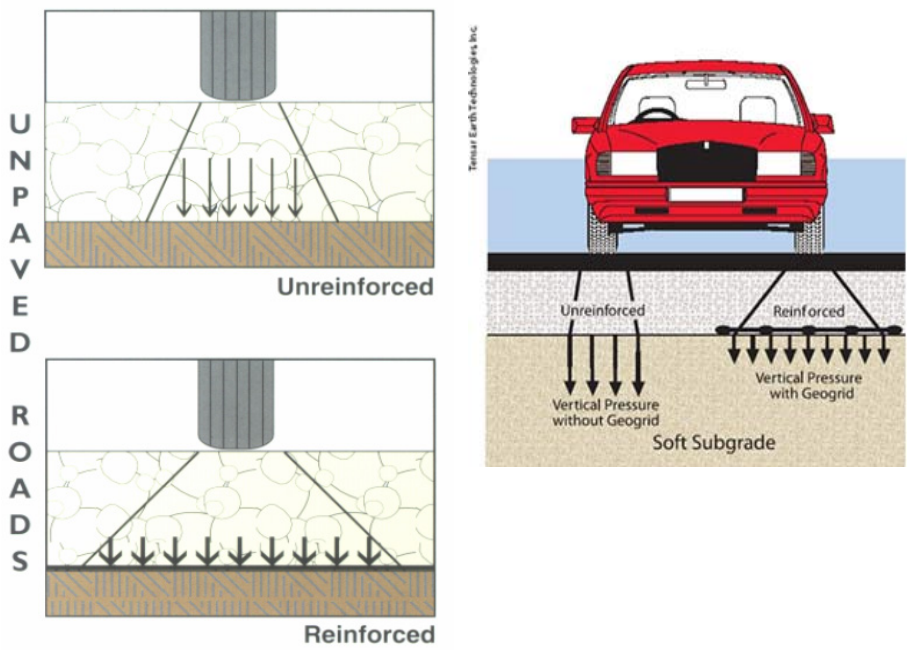


Source: Tensar International

Effectively, the lateral constraint of particles by the geogrid augments the resistance of the particles to mass transport *via* shear. Subsequently this shear resistance transfers load away from the reinforcing layer through the pavement both vertically (arrows) and horizontally (angled lines). This implies that, the conclusions reached above notwithstanding, for an aggregate/geogrid couple the geogrid apertures should be correctly matched to the aggregate in some way, either with the largest aggregate particle size, or low multiples thereof, in order to obtain best action (figure 2.7). But, it does seem that as long as there is a physical interaction between the aggregate and the geogrid, there will be an increase in shear resistance and subsequent stabilisation.

**Figure 2.7 Physical particle interlock with geogrid apertures and particles in subsequent layers**

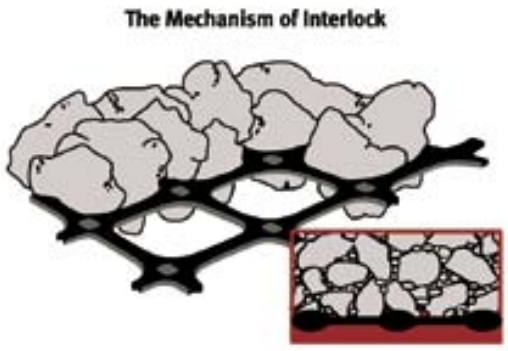


The optimal installation position of the geogrid in the pavement remains the subject of some debate. The vast majority of the work to date has been done with the geogrid at the base/sub-base interface with the idea of stabilising the sub-base (and by extension reinforcing the basecourse) rather than reinforcing the basecourse itself. However, recently undertaken studies of the placement at different positions in the basecourse other than at the basecourse/sub-base interface showed the geogrid was very effective at reducing granular material shear deformation in the traffic direction and in thin

pavements (Al-Qadi et al 2012). It was also suggested that, for thick base layers, while a single geogrid layer in the upper 1/3 of the layer would improve pavement performance, the installation of a geosynthetic stabilisation layer at the base subgrade interface may be needed for additional stability. These conclusions could be reached logically by invoking the interlock of aggregate particles above and below the geogrid thereby creating a beam rather than tensioned membrane, a theory that is invoked alongside the lateral restraint models (figure 2.8). The beam effect is discussed in the mechanisms of geocell action, but not generally in models of geogrids. However, as discussed, if the geogrid is placed within the basecourse layer so that the same materials are located both above and below the geogrid, then it may well be possible to invoke the beam effect. The tensioned membrane effect is discussed below.

**Figure 2.8 Force distribution beneath load on pavement; foundation footing load**

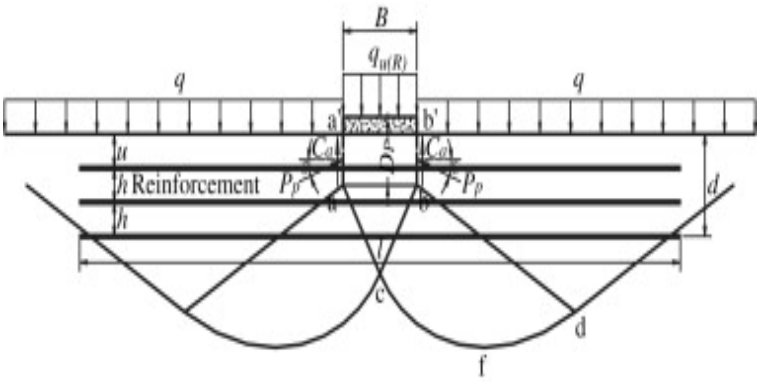


Source: Tensar International

Figure 2.8 describes the distribution of force through a pavement of a load applied in the vertical direction. This common model is typically used to describe foundation footing stress in a continuous soil matrix, but is also applied to systems such as granular basecourses. The model has been adopted by pavement engineers to describe a snapshot of a load on an unbound granular pavement, in this case with a surface layer confining stress $q$, and the 'point' stress $q_{n(R)}$ of width $B$. It shows the shear wedge ($abc$) under that load ($Bq_{u(R)}$) and the shear zones that are induced by 'penetration' of the shear wedge. The magnitude of the shear wedge is determined by the load and the nature of the matrix, with phenomena such as the angle of friction and interlock playing important roles in determining the dimensions of the different zones. Introduction of geogrid reinforcement restricts the amount of shear that would otherwise be expected to be induced by the shear wedge, thereby reducing the magnitudes of both the active (bcd) and passive Rankine shear zones and ultimately the mass transport that would otherwise occur, culminating in reduced permanent deformation (Craig 1997).

While they can be treated separately, it seems that the lateral restraint concept and the improved bearing capacity concepts cannot occur independently as they both involve reductions in material shear, or mass transport.

The tensioned membrane concept (Giroud and Noiray 1981; Giroud 1984) was introduced early into the concept of reinforced pavements. If a vertical load (stress) is introduced to the pavement, a concave shaped deformation is induced which is resisted by the geogrid reinforced matrix. The effective boundary layer created by the geogrid will resist deformation through its increased modulus. This is reflected through the entire matrix, thereby increasing the effective modulus of the pavement as a whole. It should be noted that the tensioned membrane effect (and the beam effect) cannot begin to act until a tension stress has been introduced to the geogrid (figure 2.9). This in turn means that there must be a degree of permanent deformation induced in the pavement in order to

induce that tension, as it is not possible with current methods to effectively pre-tension the geogrid *in-situ* except via the compaction mechanism. However, the tensioned membrane effect is now falling out of favour as a stabilisation mechanism.

**Figure 2.9 Schematics of the actions of the proposed reinforcement mechanisms**

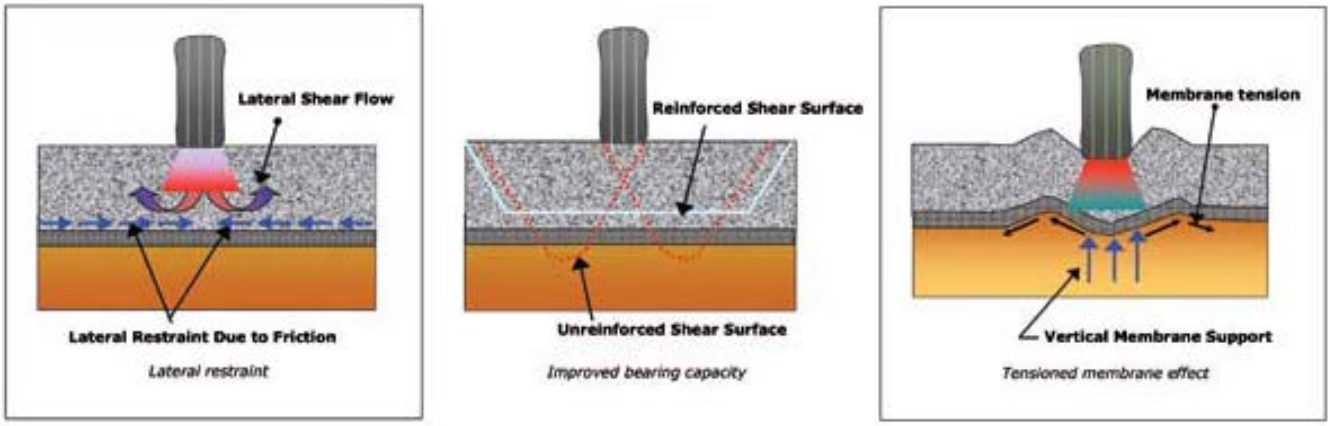


Source: Archer (2008)

The overall effect is that by restricting the ability of the aggregate particles to move, and by effectively fixing them into place *via* interaction with the geogrid, mass transfer through the pavement will be restricted. If particles cannot move then the modulus of the matrix will be maintained and the rate of accumulation of plastic deformation via shear and/or consolidation will be reduced.

## 2.3 Geocells

Somewhat less work has been done to examine the effects and mechanisms of three-dimensional geocells. However, those effects and mechanisms would seem to be similar to those of geogrids, but perhaps magnified. The three-dimensional nature of geocells (ie their physical vertical size) and their higher cost introduces constraints over how and where they might be implemented in a pavement environment. Geocells are apparently much more expensive (perhaps by factor of 50 or more) than geogrids, so it is likely their application will be limited to specialist, niche or extra high-value situations.

Geocells are effectively a three-dimensional extension of geogrids wherein a polymeric structure is created with depth in addition to width and length. Indeed, the majority of geocell products used are around 100mm or more deep, which in many cases might be of the order of 50% of the depth of a pavement basecourse (figures 2.10 and 2.11). Two major embodiments of these materials exist: 1) fixed size and shape rigid plastic cells that are supplied in various sized segments and incorporated into the site in sheets, or 2) a flexible composite material that is supplied in collapsed segments, expanded by hand, joined together in-situ and fixed into position. The aim of geocells is to isolate and then fix in position the less compactable, more mobile components of an unbound pavement or granular structure. The major area of implementation of geocells is in soil stabilisation in earthen walls, in sand and gravel stabilisation in general construction environments, and in stabilisation of very low-bearing capacity soils. In the pavements sector, geocells have seen very successful application in subgrade and sub-base stabilisation in temporary roads, such as haul roads, in areas with very low-bearing capacity soils such as swampy and sandy areas, and also in railroad ballast stabilisation. They are also becoming more widely applied in areas of low traffic but high value, such as temporary access roads, unsealed parking areas and gravel access ways to high-value sites that

would be too expensive or environmentally damaging to build otherwise. Designs of geocells differ with regard to water flow through the walls of the geocell, or only through the media contained within the cells and of course they differ in depth, cell size and material. The vast majority develop into square or diamond-shaped cells.

For pavements that include geocells, TBR values of up to 130 have been described. While this sort of value might sound optimistic for a standard high-volume pavement, in the cases of specialist pavements that have very low bearing capacity subgrades or sub-bases, improving the TBR by 130 might mean the difference between being able to actually use a road (such as access roads over swampy areas) or the road disappearing into the subgrade.

**Figure 2.10 Flexible but rigid polymer geocells expanded and anchored into place**

Source: PRS Inc

**Figure 2.11 Rigid plastic type geocell product from DIY stores for walkway/driveway applications**

A summary of previous work (Leschinsky and Ling 2013a) described the effects of geocell confinement on the behaviour of gravel in railroad construction, with the aim of reducing maintenance and increasing train speeds. While railroads are not road pavements and load distributions are line loads rather than point loads, the concepts regarding ballast particle confinement and distribution of load are generally compatible.

Stabilising the granular portion of a pavement, ie the basecourse, by geocell reinforcement distributes the stress over a much larger volume than would be the case in an unstabilised section. This has a significant impact on the effect of loads on the sub-base and subgrade of the pavement (Chrismer 1997; www.prs-med.com/index.php/road-construction/road-construction-overview; Yang 2010). In addition to the redistribution of vertical loads (stresses), the confining behaviour provided by geocell reinforcements has been shown to reduce and/or redistribute shear stresses in the sub-base (Zhou and Wen 2008) which, in the case of pavements with granular basecourses over less stabilised bases, is desirable.

The geocell layer can be described as having the effect of a rigid composite 'mattress' or 'beam' which is able to reduce or even prevent entirely, lateral spreading of soils and aggregates (Zhou and Wen 2008; Leshchinsky and Ling 2013b). Increased stiffness of granular material matrices through the use of geocells can go as far as to be compared to a slab (Pokharel et al 2011). In the case of geogrids this effect is referred to as the tensile membrane effect, but due to the depth component of the geocell, the effect is referred to as the 'beam effect', likening installation of the geocell to installation of a reinforcing beam into the pavement (figure 2.12). However, unlike geogrids, the lack of a generic design methodology for geocells, along with their higher cost, has inhibited their implementation in pavement environments (Han et al 2008).

## 2.4 Modelling of geogrids and geocells

More work is now focusing on fine tuning the use of geosynthetics, on understanding their mechanisms of action and the overall effects of their use. Much of this work has involved computational methods with researchers developing and refining models so they will better support the empirical results obtained. Finite element modelling (FEM) has become a very powerful technique in the past few years to better explain experimental observations, but researchers have been using the techniques to model the effects of geogrids for many years (Dondi 1994; Howard and Warren 2006; Yang 2010). FE models that have been developed often involve elastic-plastic material models for the asphalt layer (where appropriate), the base aggregate and the sub-base layers, and an anisotropic linear elastic model for the geosynthetic material.

Anisotropy in the elastic response of polymer materials, from which the geosynthetics are made, is consistent with the properties of their materials. More in-depth discussion of the models can be found in the references. Membrane elements can be included for the geosynthetic where those elements are capable of carrying load in tension but have no resistance to bending or compression.

**Figure 2.12 Schematic description of stress re- distribution and beam effect modulus increase in a geocell reinforced basecourse demonstrating stress distribution beam- effect**

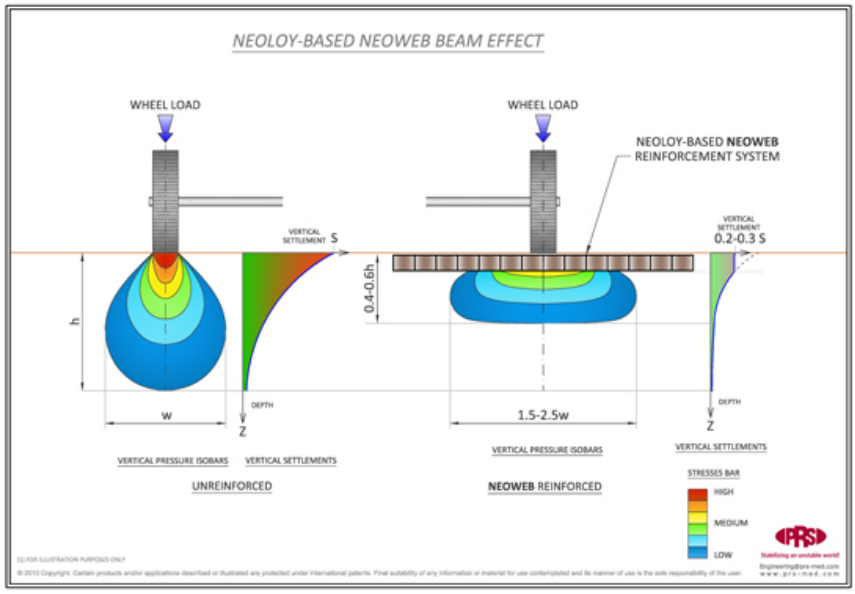


Source: PRS Inc

In early work, a geocell reinforced flexible pavement was modelled using both linear and non-linear constitutive material models (Dondi 1994). That model, which included linear elastic material models based on Hook's law, Drucker-Prager and Cam Clay models (Drucker and Prager 1952; Roscoe and Burland 1968), suggested 15–20% reduction in vertical displacement under the load in reinforced sections and 2–2.5 times increase in pavement fatigue life. Decreases in permanent deformation with a geocell at the basecourse/sub-base interface, were modelled using an axis-symmetric analysis (Howard and Warren 2006). Again, permanent deformation reduction of up to 20% was found.

Significant effort has been made by Perkins and by Giroud to provide models of geogrid reinforced pavement systems (Perkins and Edens 2002; Giroud and Han 2004). This work included distress models to describe the stress and strain responses for geogrid reinforced flexible pavements, especially for where the geogrid is placed at the bottom of the unbound aggregate layer. These models are useful in that they include membrane elements along with linear-elastic elements. Both the Perkins-Edens and the Giroud-Han models have been shown to provide general descriptions of reinforced pavements that may be consistent with those previously observed in instrumented pavement test sections.

The reinforcement effect of placement position of the geogrid in asphalt surfaced pavement using a two-dimensional axisymmetric pavement response model has been investigated (Moayedi et al 2009). The asphalt layer and geogrid were modelled as linear elastic anisotropic materials while the Moho-Coulomb material model was used to simulate granular layers, and static loads were applied. They determined that geosynthetic reinforcement added at the bottom of the asphalt layer, ie in the upper part of the basecourse, leads to the highest reduction in vertical pavement deflection. They also determined that overall performance of the pavement is improved if effective bonding is maintained between the aggregate and the geogrid.

Significant work in this area has also been produced by Tensar Corporation in collaboration with University of Illinois who have provided tools to aid with the mechanistic design of geosynthetic reinforced pavements. AASHTO has moved towards mechanistic design concepts for pavements, therefore the development of mechanistic models that include geosynthetics has become more important. Using nonlinear mechanistic models, Kwon et al compared responses predicted from isotropic and cross-anisotropic characterisations of the granular basecourse (Kwon et al 2005; Kwon and Tutumluer 2009; Kwon et al 2009). They determined that the use of high-stiffness geogrid reinforcement reduced critical pavement responses, and that stiffening of the granular base and the sub-base layers reflected in the slightly increased values for the modulus in the vicinity of the geogrid. They produced the simple, yet effective description of confinement zones within the pavement extending away from the geogrid (figure 2.13).

An issue in the New Zealand context perhaps, lies in the uppermost 'unconfined' zone. Where an asphalt concrete is used as the surface this unconfined zone becomes confined by the asphalt. Where a chipseal is used, the magnitude of the surfacing induced confinement is much reduced, thereby increasing the propensity for shear or consolidation in that unconfined zone.

**Figure 2.13 Representation of the zones and magnitude of confinement in a granular pavement**

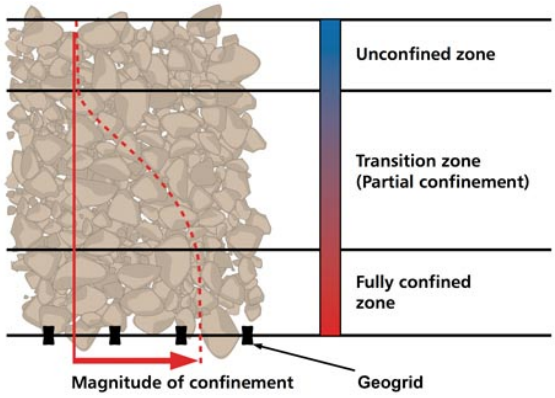


Source: Cavanaugh and Kwon 2008.

FEM has also been used to analyse the effect of geogrid base reinforcement on flexible pavements. The analysis investigated geogrid placement only at the basecourse/sub-base interface and the conclusions reached were similar to previous ones. They are summarised below (Abu-Farsakh et al 2014):

- The use of geogrid base reinforcement results in reduction of the lateral strains within the basecourse and subgrade layers, reduction of the vertical strain and shear strain at the top of the subgrade, and reduction of the surface permanent deformation (through the stabilisation of layers below the surface).
- The reductions in developed strains through inclusion of geogrid were more appreciable in sections with weak subgrades compared with those in sections with stiff subgrades
- The benefits were reduced as the thickness of the basecourse layer increased and were enhanced as the tensile modulus of the geogrid layer increased.
- The increase in geogrid tensile modulus resulted in significant reduction of surface permanent deformation. However, the effect of geogrid tensile modulus decreased with the increase in the thickness of the reinforced basecourse layer and increase in sub-base strength.

- The results of mechanistic-empirical analyses showed that the predicted service life of pavement structure in terms of TBR can be significantly increased with the inclusion of geogrid base reinforcement in the pavement structure. The TBR values can reach as high as 3.7 for thin base pavement sections built over weak subgrades using high-tensile modulus geogrids.

A small number of researchers have applied discrete element modelling methods to the granular pavement/geogrid problem. Analyses indicate that a 'stiffened zone' develops on both sides of the geogrid during compaction and traffic loading, due to the geogrid-aggregate interlock. As a result of increased contact forces and stresses around the geogrid, the stiffness of the adjacent unbound aggregate increases significantly and improves the overall pavement performance. The work showed that residual stress and confinement effects must be considered in numerical analyses and can be accounted for by assigning some initial distribution of stress horizontally around the geogrid (Kwon et al 2008). Discrete element modelling also demonstrates that the load distribution occurs in lines through the aggregate skeleton, rather than simply via the matrix (eg figure 2.14).

**Figure 2.14 Discrete element model of vertical stresses (black) in granular pavement reinforced by geogrid (red)**

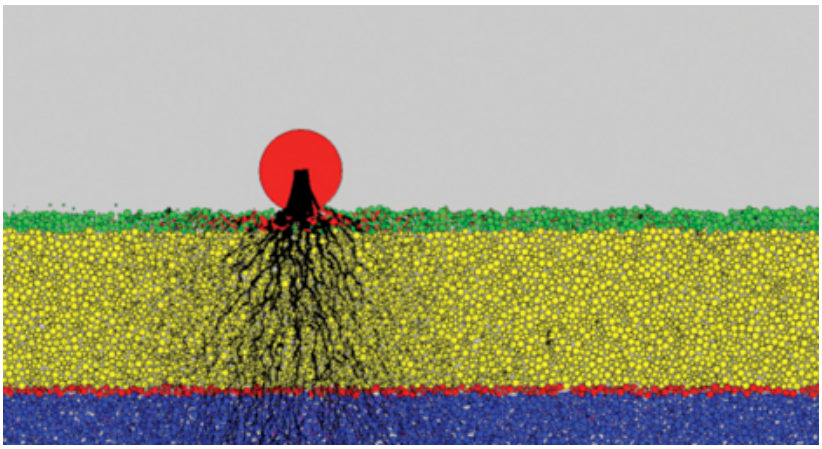

Source: Cavanaugh and Kwon 2008

Further to that study, Bhandari et al (2014) have also investigated discrete element modelling of geogrid reinforcement of basecourse. They found that improvements to the performance in both paved and unpaved roads were possible with geogrid installation. They found also that the interaction of the geogrid with the base aggregate is critical to the improved performance where, under a heavier load, the geogrid placed at the mid-depth of the base performed better than that placed at the bottom of the base, in contrast to other studies. The numerical results showed that geogrid helped widen the distribution of contact force chains and mobilised its tensile strength. The geogrid increased the load capacity and elastic deformation and reduced the plastic deformation of the base course by providing both lateral and vertical confinements (Bhandari et al 2014).

## 2.5 Design methodologies

Current practices for geogrid-reinforced pavement design methods in both AASHTO and Austroads are based on long-standing empirically derived design methods that are based on work done in the 1970s (Seward et al 1977). The TBR-based design approach, such as Practice PP46-01 of AASHTO (AASHTO 2005) provides a simple, yet limited approach to quantifying geosynthetic performance benefits (Kwon and Tutumluer 2009). AASHTO has offered guidance on moving towards more mechanistic methods based on work that has combined mechanistic methods with empirical observations. Effort is now being expended into

developing pavement design methods that can incorporate the performance properties of geosynthetic materials into both CIRCLY and Austroads design programmes and approaches. Purely empirical methods utilising rule of thumb factors (eg the 10 x CBR rule of thumb) therefore are being replaced with these new more analytical models and methods (Perkins 2001; Kwon at al 2005; Kwon et al 2009; Kwon and Tutumluer 2009; Abu-Farsakh 2014) with many of the results being based on the Perkins/Edens model (Perkins and Edens 2002; Perkins and Edens 2003) with extension by the Giroud-Han model (Giroud and Han 2004). Around the same time, the US Army Corps of Engineers published a design method considering the use of geogrids and geotextiles for paved and unpaved roads (US Army Corps of Engineers 2003). Its approach for unpaved surfaces, based on the methodology originally developed by the US Forest Service, distinguished the performance of geotextiles and geogrids as reinforcement components in subgrade improvement applications. The design charts developed by the Corps were based on empirical data obtained from full-scale test sections undertaken at the Corps Research and Development Center. This data was combined with the old bearing-capacity design methodology developed for the US Forest Service (Seward et al 1977). Based upon the Corps' independent, full-scale testing, a material specification was developed for geotextile and geogrid products (Webster 1992).

Interestingly however, a current text on pavement analysis and design (Huang 2004) introduced geotextiles only in the area of drainage filtration materials aimed at separating sub-base and basecourse. This text is quite theoretical in its approach, but makes no mention of geogrids/cells in the construction or design methods for pavements. While that text is of course not very recent, it could well suggest the application of geogrids and geocells has not yet truly reached the stage of being part of mainstream pavement design. But both Perkins (2014) and Wayne (2015) indicate that modules for the design inclusion of geosynthetics are being, or have already been developed for both CIRCLY and Austroads.

Some work has been undertaken in several laboratories in an attempt to integrate the work previously mentioned with new concepts (Kief et al 2014; Han et al 2013). One of the new concepts is called modulus improvement factor (MIF) which is an inclusive term that integrates all of the associated effects resulting from the incorporation of geocells into a pavement. Laboratory and field and FE studies were carried out to quantify the structural contribution of the geocells to pavement design. Quantification of the MIF is based on two parameters in the mechanical-empirical design methodology discussed above:

1 Traffic intensity

2 Design CBR value of the subgrade.

Significant effort in the development of mechanistic models is also being expended by the manufacturers of the geosynthetic systems themselves and while much of this work remains confidential it is being released at industry seminars and in publications.

# 3 Experimental

The objectives of this project were to examine the effectiveness against shear, of adding geosynthetic materials to basecourse materials that were compromised in terms of either their geology or their particle size/shape. From here onwards the terms ‘stabilised’ and ‘unstabilised’ will be used rather than ‘reinforced’ or ‘unreinforced’. This is to follow the growing consensus in the industry that geosynthetics serve to stabilise against particle movement rather than to add specific strength to the pavement.

The aggregate material chosen to investigate was a greywacke gravel aggregate denoted River Run. This was supplied to Opus Research by the Transport Agency’s Canterbury Accelerated Pavement Testing Facility (CAPTIF). This aggregate consisted of almost exclusively unfractured round river plain stone from the Canterbury area of New Zealand, mixed with autogenous non-plastic sand. The samples supplied were excavated, screeded and bagged. No further processing was performed. Particle sizes ranged from approximately 35mm stones to fine sand (figure 3.1).

**Figure 3.1 River Run gravel aggregate grading showing significant fine content**

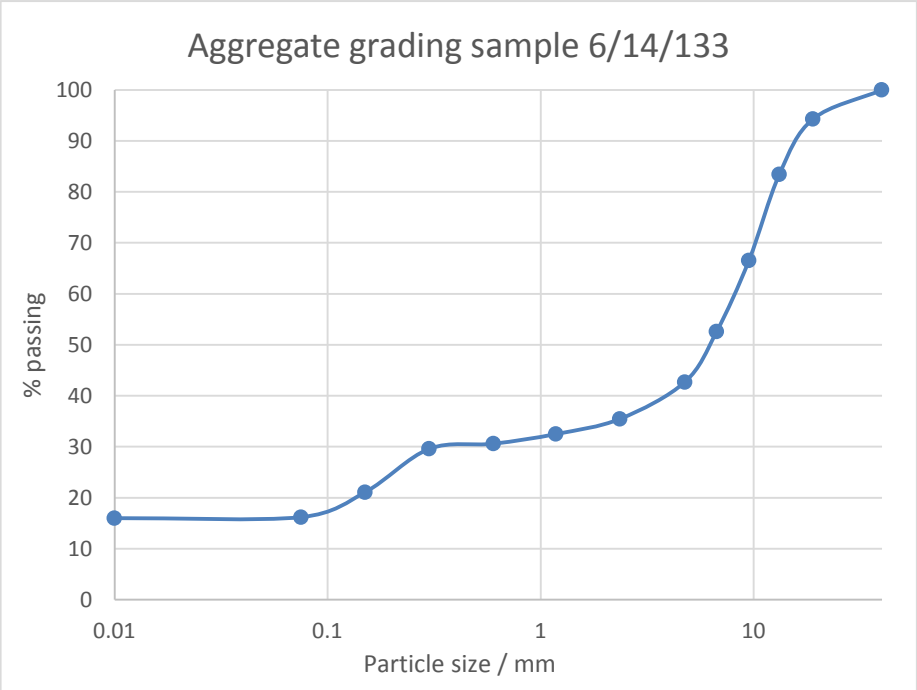


## 3.1 Repeated load tri-axial (RLT) testing

### 3.1.1 Material description

Steering committee discussion indicated that RLT testing of the material, as originally planned, was not necessary. A contract variation was approved in respect of that. Following this variation, however, a collaborator kindly offered to analyse the sample via RLT testing at no cost to the project, so this offer was accepted. Hence the inclusion of RLT analysis in this report. A sample of the River Run aggregate material was shipped to Tensar International Corporation (GA, USA) in three five-gallon plastic buckets. These buckets were representative of the larger quantities of aggregate material supplied by CAPTIF. The material has been screened only and is designated River Run.

### 3.1.2 RLT tests

In order to determine the effects of geogrid on the aggregate behaviour under repeated loads, RLT tests were conducted in accordance with procedures contained within the test standard BS EN 13286-7:2004 (British Standards Institution 2004), with the Precision Unbound Material Analyzer (PUMA). The PUMA test procedure is of value to generate comparisons between stabilised and non-stabilised aggregate properties. The data obtained should not be used to determine performance characteristics for geogrids in pavement design. Design parameters should always be determined from large-scale testing and validated by full scale accelerated pavement testing.

The PUMA equipment is shown in figure 3.2. It tests a sample of 150mm diameter and 150mm height, confined within eight curved-wall segments. The specimen was compacted in three 50mm lifts with 56 hammer drops each using a modified proctor hammer. The specimen was then loaded on its top surface by the circular platen for RLT testing in accordance with BS EN 13286-7:2004. The side walls were confined within a rubber-lined steel band, the rubber providing the possibility of wall movement under load, simulating the elasticity of surrounding material in-situ. Thus, while only vertical stress was controlled, vertical and horizontal stress and strain were all monitored during the test.

**Figure 3.2 Precision unbound material analyser (PUMA)**


As such, two specimens were prepared without a geogrid (control) and two were prepared with a large aperture tri-axial geogrid (approximately 60mm aperture size), placed in the sample at mid-height (75mm). Laboratory specimens were prepared with dry densities of 1.99tm$^{-3}$ and 2.335tm$^{-3}$ (shown as 4% moisture as provided by the supplier, CAPTIF, as optimal moisture content). This is shown in figures 3.3a and 3.3b.

**Figure 3.3 Aggregate samples before placement in tri- axial cell**

(a) Dry sample, 1.99tm$^{-3}$

(b) Moisture conditioned sample, 2.335tm$^{-3}$

The modulus of an unbound material is dependent on the stress conditions to which it is subjected. To simulate in-situ stress conditions, each specimen was loaded in three stages, with 1,000 load applications during each stage; the three vertical stress levels used in testing ranged from 20kPa to 80kPa (20kNm$^{-1}$ to 80kNm$^{-1}$). At each static stress state, deviator stresses were applied to the specimen and resilient strains were measured and recorded. Confining and vertical stresses were utilised in the calculation of the stiffness modulus at each stress state.

### 3.1.3 Stiffness modulus

The stress conditions applied to a specimen in this test are believed to be similar in nature to the stresses applied to the base layer of a pavement during trafficking. At each stage, the aggregate fills exhibited stress hardening or stiffening behaviour as shown in figure 3.4. Note that in the two graphs of the experimental

data (figures 3.4 and 3.6) there appears to be a discontinuity in the centre of each 'stage'. This appears at first glance as if extra load may have been applied resulting in further deformation. In fact it is due to an artefact of the PUMA software in that the intervals between data points are not evenly spaced. This creates the appearance of an effect, when it is actually a simple consequence of a data discontinuity.

**Figure 3.4 Resilient moduli measured from PUMA tests for dry, moist and stabilised samples**

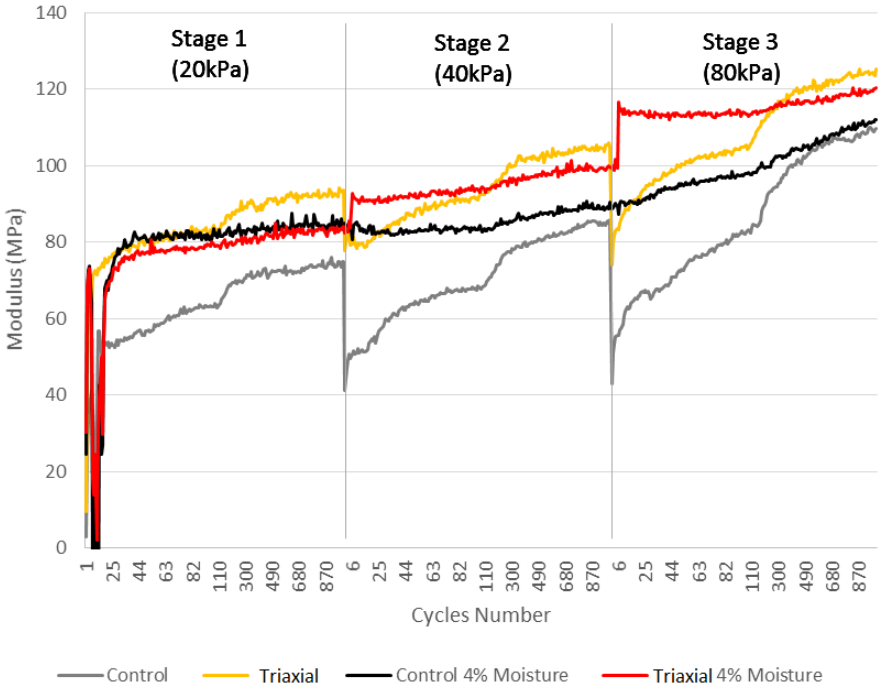


For this project, it was found to be useful to plot the average modulus in graphical form to compare values. In this case, aggregate samples with and without grid reinforcement were plotted at two different density levels (dry and moist). Figure 3.5 illustrates the average resilient modulus of each sample in graphical form.

**Figure 3.5 Average resilient modulus measured from PUMA tests**

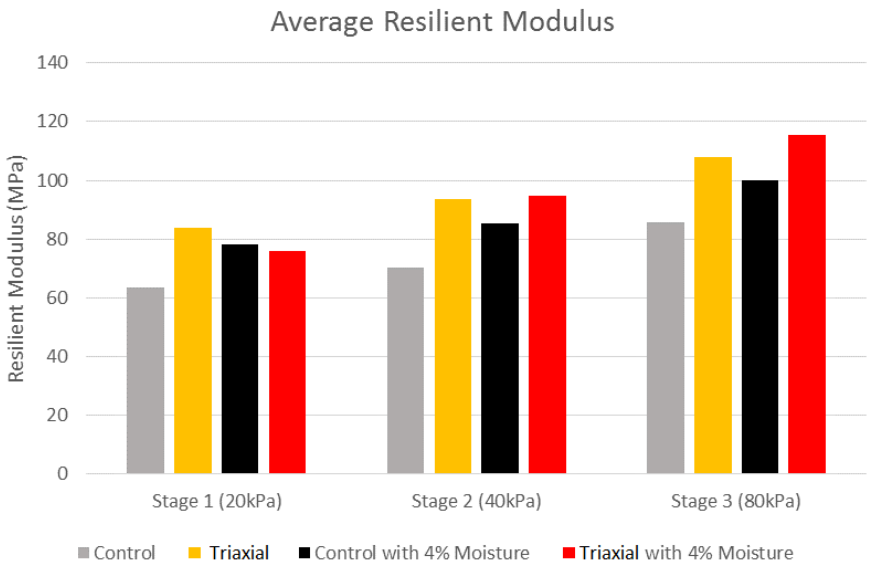

Figures 3.4 and 3.5 graphically depict the results of this test and demonstrate clearly the positive influence of the geogrid on the resilient moduli of the aggregate fills. The resilient modulus of the aggregate material was improved by 15–30% through incorporation of the geogrid at mid-height of the sample. The data also shows the influence of density and moisture content on the bearing strength of the material, with higher density samples (ie moist) exhibiting improved bearing strength.

### 3.1.4 Permanent deformation

The results presented in figure 3.6 show the measured accumulated permanent deformation of the specimens. The permanent deformation of the unbound granular material was strongly affected by the relative dry density of the material. This relative comparison indicates that the geogrid provides a greater resistance to permanent deformation compared with the same material without the geogrid. The permanent deformation was reduced by over 50% in the stabilised samples, while the increase in modulus was smaller than this, as indicated above. This result reinforces the notion that the resilient modulus of the aggregate should not be used alone as an indicator of potential rutting performance of aggregate base layers, especially those constructed with this particular material.

**Figure 3.6 Repeated load permanent deformation**

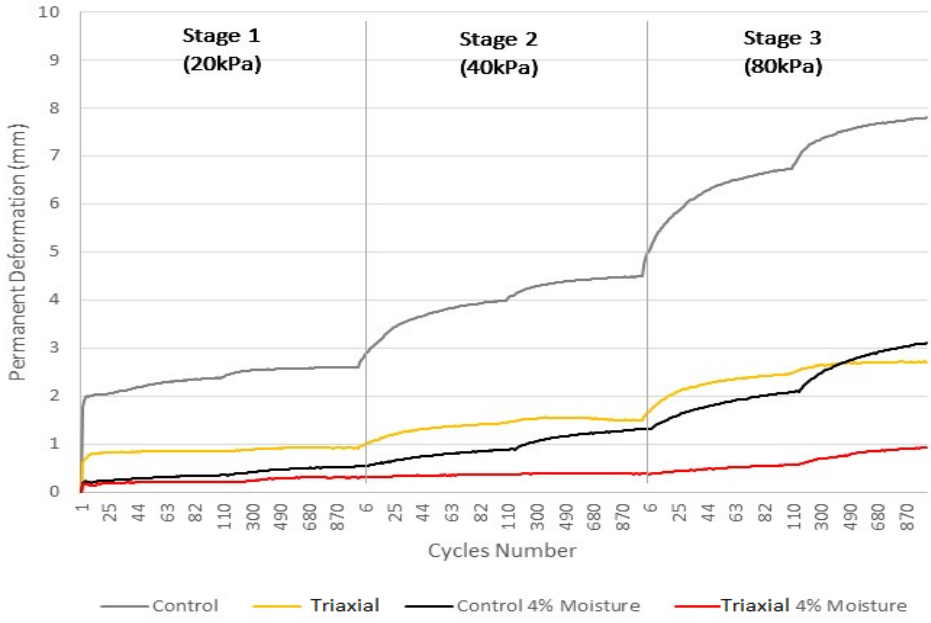


## 3.2 Wheel tracking

The approximate mass of aggregate required to fill the Opus Research Accelerated Pavement Tester (ORAPT) sample compartment (approx. 2.0T) was moistened and mixed with a Bobcat digger so as to achieve an appropriate moisture content. The aggregate sample was then loaded with the Kanga loader into the ORAPT sample compartment, which is 1.7m x 1.7m x 0.25m deep with steel side walls and a thick plywood base (figure 3.7). The aggregate sample was levelled just above the top of the sidewalls so as to allow for densification during compaction. The ORAPT instrument and experiment has been described previously (Patrick et al 2011).

**Figure 3.7 ORAPT River Run aggregate sample preparation, loading, compaction and weighing**

All samples were compacted as single lifts and compaction was achieved with a mixture of tamping rammer compaction to start the process, followed by pedestrian 660kg vibrating roller across the sample to complete the compaction. The sample exhibited significant flow characteristics during the early part of the compaction and would not accept the rolling drum compactor early on. However, as the compaction effort was initiated by the plate compactor and progressed, more interlock was established and the vibrating roller could be brought to bear (figure 3.7). Platforms were constructed on either side of the sample tray enabling the roller to be rolled off the sample so that reversing and manoeuvring of the roller was not done on the top of the aggregate sample itself. Using the nuclear density meter (NDM), the

appropriate degree of compaction was established (see tables below). Note that while this sample preparation method does not necessarily match the granular basecourse construction standard described in NZTA B2/02:2005 (NZ Transport Agency 2005), it was achievable in our experiment, is used consistently and allows for reproducible sample compaction for comparative purposes.

The surface of the sample did not develop a hard crust-like structure as is generally observed in a typical M/4 aggregate. But it did end up becoming dense enough so that a person could walk on it, albeit carefully, without badly disturbing the surface of the sample. It was also noted that the uppermost surface could be lightly brushed off to leave a tougher, more compact surface. However, if this was left to dry out, as in the case of sample 1, the surface became very loose and mobile. But if an appropriate level of moisture was maintained, as for later samples, it remained tough and compacted. The role of moisture in improving the stability of the aggregate matrix is supported by the RLT test results discussed in section 3.1.

**Figure 3.8 ORAPT wheel tracking device with sample tray in position**

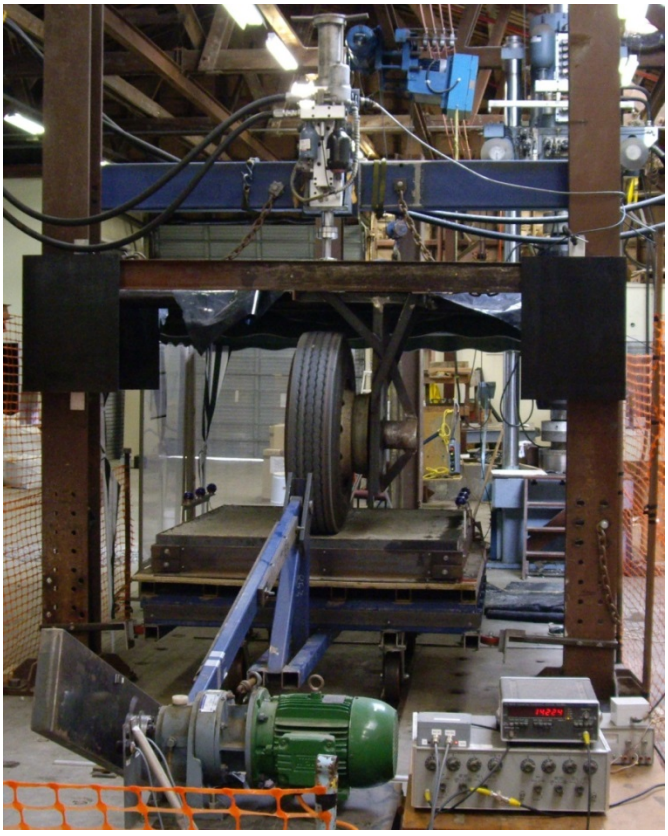

The ORAPT device (figure 3.8) is constructed so the sample compartment is traversed in a reciprocating manner beneath an Austroads standard truck wheel/tyre combination, which is pressed down onto the sample. The load applied by the wheel to the sample is controlled precisely by a computerised high-pressure hydraulic system. The load could be applied so the wheel was in contact with the sample in both directions, or in one direction only, to replicate the movement of traffic over an area of pavement. The latter procedure was used here.

The speed of the sample for each pass was maintained at 0.5ms$^{-1}$ and the total length of the sample contact path was 1.5m. For the first 0–5,000 passes, measurements were made after each 100–500 passes; from approximately 5,000 passes onwards the sample was tracked for longer periods, pausing to take measurements after approximately every 1,000–2,000 passes. More frequent measurements were

made early in order to capture early deformation of the sample.

## 3.3 Surface deformation ‘rut’ measurement

The accumulation of surface deformation was captured using a laser and photograph system (figures 3.9 and 3.10). The deformation and rut formation were then analysed and determined using an image analysis system in MATLAB software. Two laser beams were fixed at the edges of the middle of the sample tray (corresponding to the centre and most affected part of the wheel path) and aligned so as to provide a single line, normal to the wheel path. A fixed length and height reference bar was placed parallel to and above the laser line and a digital photograph was taken. The photograph was then analysed where the laser line and reference bar were identified and the positions of the laser line, which followed the rut surface, and the reference bar were established relative to one another. The shape of the deformation was thus discovered and from this it was possible to measure the total depth of the deformation, or rut that had formed during the wheel tracking.

**Figure 3.9 Sample 1. Example of laser line over ORAPT sample surface including datum bar and reference points. Image taken at 0 passes prior to wheel tracking. Note that the surface is typically not perfectly flat following compaction**

The distinction between ‘surface deformation’ and ‘rut’ is made here, where the former describes simply the fact that the surface had been deformed in some way, while the latter describes specific deformation, which is measured from a line between the two highest points of that deformation (shoulders) to the lowest part of the deformation (wheel path). The combination of the two aspects, shoulder and wheel path, constitutes the ‘rut’. Here we took the highest points of the shoulders along the laser line and the average of the centre of the deepest part of the wheel path. The Y-axis error bars in the graphs of rut-depth represent the apparent uncertainty in the measurement (± 5mm) rather than a statistical analysis of rut depth values, due to the data arising from one measurement only.

**Figure 3.10 Sample 1 after 540 passes showing laser line and datum bar across rut formed in sample. Note taller shoulder on right- hand side of rut probably due to a misalignment of the wheel load**

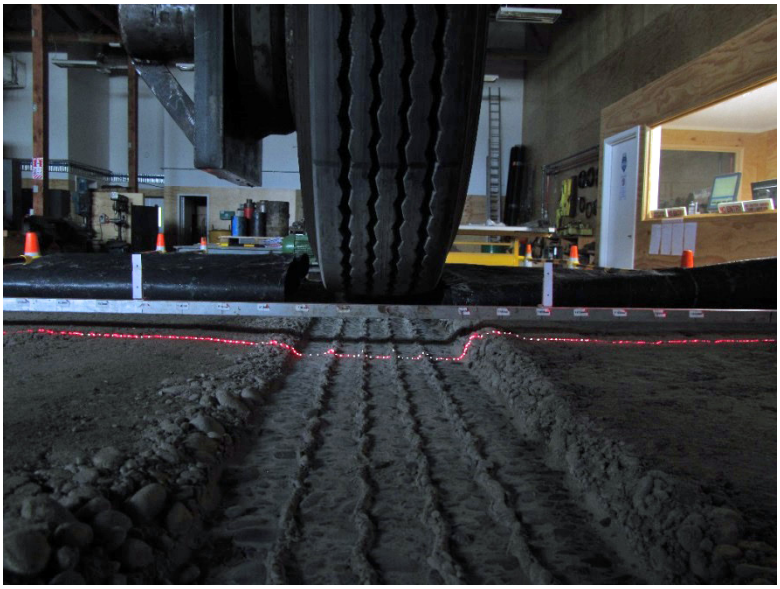

## 3.4 Unstabilised samples

In order to establish the optimal experimental conditions and of course also to identify the behaviour of the River Run supplied aggregate, three unstabilised samples were prepared and tested in the ORAPT device. Sample 1 was a bare, compacted sample with no wearing course or moisture sealing layer. Sample 2 had a 20mm thick cold-mix asphalt wearing course and sealing layer on the top surface of the sample, while sample 3 had two changes. A 25mm thick neoprene rubber sheet, with Shore hardness of 60A (approximate Youngs modulus, $E$= 2.15 MPa), was placed on top of the plywood base (figure 3.11) and an emulsion grade 3/5 'racked-in' chipseal was added to the top surface of the sample as a wearing and moisture sealing layer.

**Figure 3.11 ORAPT sample container, with the rubber (Shore 60A, E ≈ 2.15MPa) model sub- base fitted**

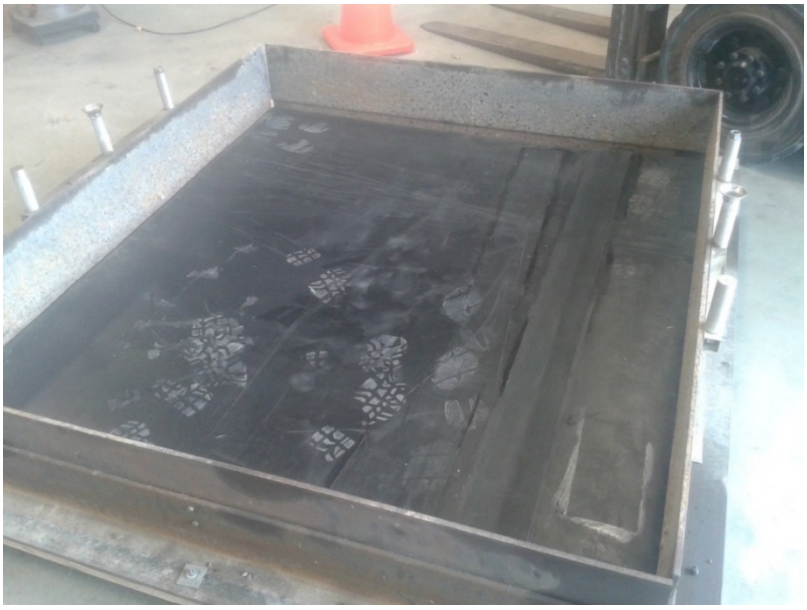

The use of a hard rubber base has been established elsewhere as a practical method of modelling a good quality (high CBR) sub-base beneath a basecourse sample, without having to actually construct a sub-base (Das and Chodhury 2015).

### 3.4.1 Sample 1 – no surface treatment

The construction of this sample followed the same basic procedure of several previously constructed on the ORAPT facility. It was assembled on the plywood base of the sample tray and had no wearing/sealing course on the surface. Table 3.1 provides the results of NDM measurements to calculate the degree of compaction of the sample prior to wheel tracking. The results indicate that the compaction achieved in our sample is comparable to results at CAPTIF and to other materials. A load of 20kN was applied via the ORAPT tyre to the sample and tracking was in one direction only. The lack of wearing course allowed the ORAPT tyre to cause immediate deformation of the surface under the tyre. Simultaneously, even though the sample was kept covered with plastic sheets when not being wheel-tracked, the sample appeared to dry out very quickly requiring periodic re-moisturising of its surface.

The sample began to develop a surface deformation almost immediately, which developed rapidly into an obvious rut (figure 3.10). The progression of the rut formation is presented in figure 3.12. However, this data under-represents the complete rut formation, because due to the dryness of the sample and lack of wearing course to glue the surface together, the top edges of the rut shoulder collapsed continuously during the trial so that it was not possible to measure the 'true' depth of the rut. The rut-depth data therefore suggests the rut formation reached a semi-steady state that was not, in fact, the case. A certain degree of compaction by the tyre was observed in the wheel path, but the most obvious observation was the deformation caused in the basecourse sample by the wheel tracking. Tracking of this sample was terminated after 58,000 passes as the rut formation was obvious and becoming too deep to maintain safe wheel passage.

**Table 3.1 Density and moisture content calculations from NDM measurements: sample 1**

| Spot | WD ± 50 | DD ± 50 | % M ± 0.2% | % Comp ± 2 |
|---|---|---|---|---|
| 1 | 2,334 | 2,237 | 4.1 | 96 |
| 2 | 2,342 | 2,242 | 4.3 | 96 |
| 3 | 2,318 | 2,225 | 4.0 | 95 |
| 4 | 2,354 | 2,266 | 3.9 | 97 |
| 5 | 2,346 | 2,247 | 4.2 | 96 |
| 6 | 2,341 | 2,250 | 3.9 | 96 |

The conclusions reached were that the basecourse material exhibited very little shear resistance and that the moisture needed retaining via a wearing course. It was decided, therefore, to test the material with an asphalt wearing course.

**Figure 3.12 Rate of rut formation of unsurfaced, unstabilised sample**

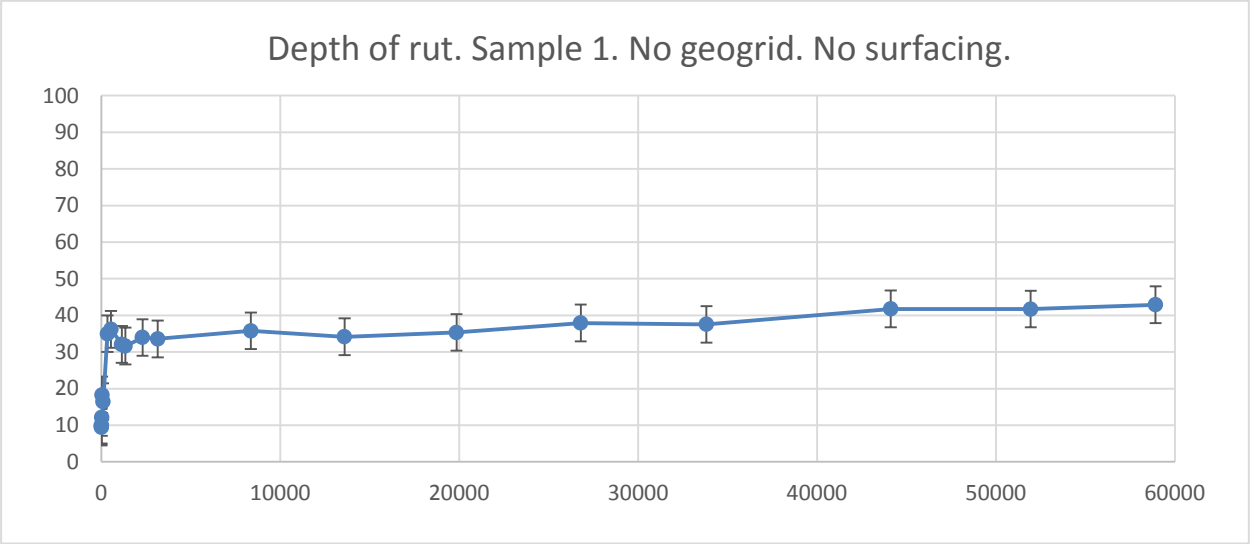


## 3.4.2 Sample 2 – asphalt surface treatment

In order to better maintain the moisture content of the sample and also to provide a more resilient surface on which the tyre could run, a 20mm thick cold-mix asphalt layer (EZ-Street) was laid onto sample 2 (figure 3.13). This sample was in all other aspects the same as sample 1. Density and compaction data (of the basecourse prior to application of the asphalt layer) are presented in table 3.2.The asphalt was laid by hand and followed by roller compaction as per the manufacturer's specifications. The sample basecourse accepted the asphalt layer with no problems of shear or collapse.

**Table 3.2 Density and moisture content calculations from NDM measurements: sample 2**

| Spot | WD ± 50 | DD ± 50 | % M ± 0.2% | % Comp ± 2 |
|---|---|---|---|---|
| 1 | 2,314 | 2,224 | 3.9 | 95 |
| 2 | 2,339 | 2,238 | 4.3 | 96 |
| 3 | 2,321 | 2,228 | 4.0 | 95 |
| 4 | 2,359 | 2,272 | 3.7 | 97 |
| 5 | 2,346 | 2,247 | 4.2 | 96 |
| 6 | 2,326 | 2,238 | 3.8 | 96 |

**Figure 3.13 Sample 2. EZ- street cold mix asphalt surface**

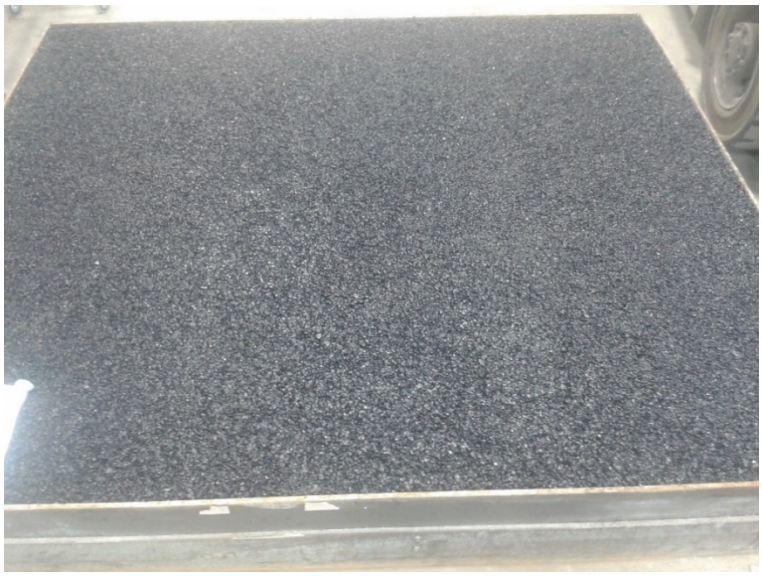

The wheel load was again 20kN. A very square-shaped rut developed in the asphalt and continued to develop until approximately 22mm deep. This rut was uniform in shape at the sides, with square edges with no shouldering and was therefore thought to be due only to compaction of the asphalt beneath the tyre. However, after approximately 100,000 passes the tyre began to have difficulty moving freely within the rut channel and the trial was terminated. The graph of the rate of rut formation in figure 3.14 showed very rapid deformation up to approximately 5,000 passes, followed by continued but very much slower rate of rut formation from 7,000 to 100,000 passes. It seems reasonable to suggest there were possibly two different processes occurring either simultaneously or in succession with different deformation rates. The first process, asphalt rutting, resulted in rapid deformation to approximately 18mm and the second, basecourse rutting, in deformation of approximately 4mm.

**Figure 3.14 Rate of rut formation of asphalt surfaced, unstabilised sample**

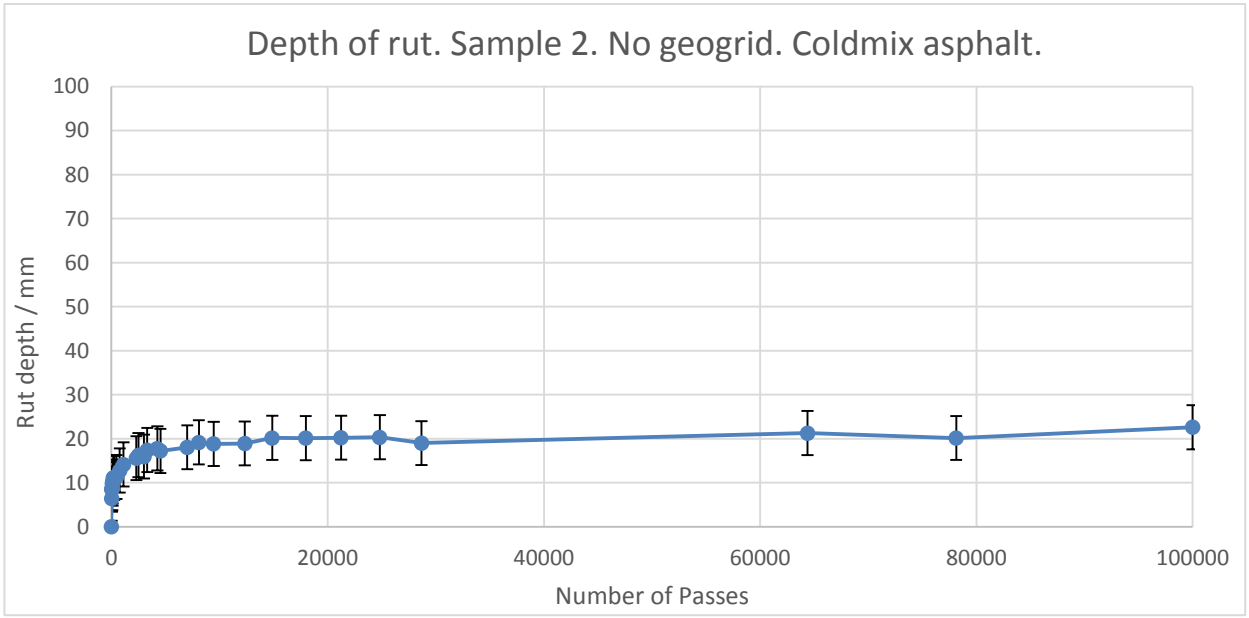

Following termination of wheel tracking, the sample was sectioned along the same path as the laser line, across the middle of the sample (figure 3.15). The basecourse material was dug out of the tray at one end so as to examine the behaviour of the asphalt and pavement through the section, which was possible because the asphalt was holding the surface of the sample together. The asphalt under the wheel path had become significantly more compacted than the asphalt elsewhere and appeared to have contributed to the majority of the rut. It was also clear there had been some compaction and possible shearing of the pavement material that also contributed to the rut. The shape of the rut was not symmetric, with one side being deeper than the other. It is likely this was a result of misalignment of the load of the ORAPT device as the same asymmetry was observed in all samples.

It was not possible to determine unequivocally if the asphalt and pavement deformation had occurred simultaneously, or if the wheel load had caused the asphalt to achieve a maximum density and then to subsequently begin to consolidate or shear the basecourse. However, the graph of rut depth data in figure 3.14 does perhaps suggest two different and sequential processes.

The conclusion drawn therefore was that the asphalt layer, in the context of this experiment, was adding too much strength to the surface of the pavement sample to allow accelerated testing of the basecourse. It was also concluded that application of an asphalt layer on this River Run aggregate might offer some promise of real-world utility. In the context of this experiment, however, there remained a need to provide a moisture sealing layer and a wearing layer on the sample, but one that would allow observation of deformation in the basecourse. It was therefore decided to trial a grade 3/5 chipseal surface on the surface of sample 3 as a compromise between the strength of the asphalt and the moisture sealing function of the chipseal.

**Figure 3.15 Section through sample 2 surface after 100,000 passes showing greater depth on one side, compaction of the asphalt and slight shear of the basecourse**

### 3.4.3 Sample 3 – chipseal surface treatment

At the same time as sample 2 was being completed and prior to sample 3, Opus Research received a visit from the technical manager of an international geosynthetic manufacturer. This programme and experimental approach were discussed and it was concluded that the use of the plywood base on the

sample tray was not ideal because rather than modelling a sub-base with a finite bearing capacity, the plywood base modelled a sub-base with effectively infinite bearing capacity, at least in the context of this system. A different base that modelled a sub-base with 'good' bearing capacity and modulus would be preferable. It was suggested that testing be continued with a rubber base in place that would model the modulus of a high-quality sub-base. A base of 25mm Shore 60A neoprene rubber was sourced and installed prior to adding and compacting the aggregate for sample 3 (see figure 3.11). In this sample, the initial compaction proved to be slightly more difficult than the previous samples, but once the compaction effort had taken hold, the compaction proceeded as with previous samples (table 3.3).

**Table 3.3 Density and moisture content calculations from NDM measurements: sample 3**

| Spot | WD ± 50 | DD ± 50 | % M ± 0.2% | % Comp ± 2 |
|---|---|---|---|---|
| 1 | 2,318 | 2,232 | 3.7 | 95 |
| 2 | 2,406 | 2,300 | 4.4 | 98 |
| 3 | 2,359 | 2,265 | 4.0 | 97 |
| 4 | 2,326 | 2,258 | 4.2 | 95 |
| 5 | 2,342 | 2,248 | 4.0 | 96 |
| 6 | 2,302 | 2,212 | 3.9 | 95 |

The chipseal was applied by spreading a 60% primecoat emulsion (180/200 pen grade bitumen) over the surface of the sample, followed by grade 3 chip and finally grade 5 chip to prepare an approximation to a grade 3/5 racked-in seal (figure 3.16). The chips were rolled in with a light roller (hand roller, approximately 20kg). The chipseal was left for two days to allow the emulsion to break completely, excess chips removed and wheel tracking commenced.

Surface deformation was observed very quickly, and included both a depression in the wheel path and raising of shoulders on both sides of the wheel path. The depth of the rut and height of the shoulders progressed quickly as wheel tracking continued and was virtually identical to the behaviour of sample 1. In this case however, because the surface was being held together by the chipseal, the top surface and edges of the shoulders did not collapse, so we were able to obtain more accurate measures of the total rut depth (figure 3.17). It was noted that shoulder formation proceeded very slightly further on one side of the rut than the other. This follows the observation made in sample 2 of the asymmetry of the rut and further indicates non-alignment of the wheel load.

Figure 3.18 displays the graph of the rate of rut formation. This data follows a typical trend of rapid deformation which slows and transforms into a slower, perhaps linear rate. The second part of the rate curve appears to be steeper than that observed in the data from sample 2, but it must be recognised that at 7,000 passes the rut in sample 2 was still in the rapid formation region of the graph. This, however, is further evidence that the asphalt layer on sample 2 offered significant reinforcement to the sample and thereby slowed the rate of rut formation.

This experiment was terminated prior to the planned number of passes due to the rapid rate of rut formation.

**Figure 3.16 Sample 3, grade 3/5 emulsion chipseal**

**Figure 3.17 Sample 3, rut formed after 7,000 passes at 20kN load**

**Figure 3.18 Rate of rut formation of chipseal surfaced, unstabilised sample**

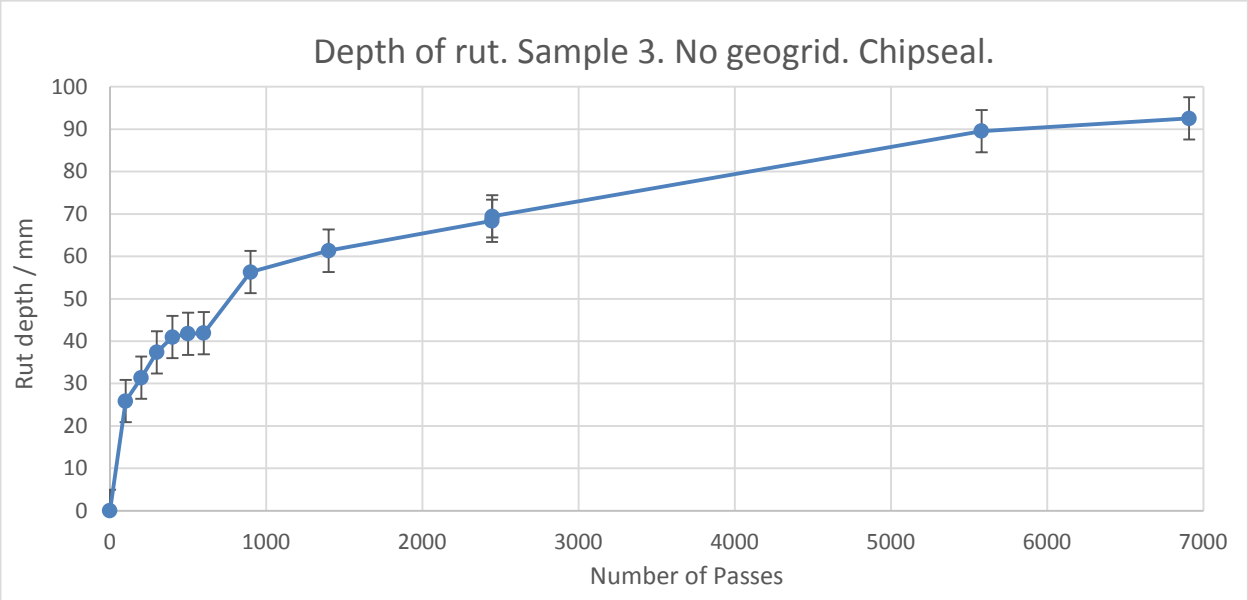


The chipseal could be peeled off the surface of the sample very easily by hand, so the basecourse sample could be recycled (figure 3.19). The ease with which the chipseal was removed does raise possible questions regarding the strength and the long-term integrity of the chipseal/basecourse interface. Due to the poor stone mosaic surface created with this aggregate material, the surface of the basecourse had limited integrity and was easily removed. Thus, when the chipseal emulsion was added it only penetrated the first few millimetres of the surface. For removal of the chipseal, the cohesion in the bitumen layer was sufficient for it to remain intact and to take the first few millimetres of the surface with it as it was removed. The remainder of the sample remained undisturbed. It is also clear from figure 3.19 that the moisture of the sample was readily retained by the chipseal.

**Figure 3.19 Sample 3, removal of chipseal**

Following removal of the basecourse material we were able to examine the rubber base for damage (figure 3.20) where no damage was found, which suggested that the rubber base and aggregate systems were compatible.

**Figure 3.20 Rubber base after use with aggregate removed**

The conclusions reached from sample 3 were that the rubber base survived in this experiment and its use would continue. The rate of rutting/deformation was basically the same as that without the rubber base, but its incorporation was more theoretically robust than a solid wood base. The chipseal provided a useful wearing course without providing too much, if any, strength to the surface and it maintained the moisture content of the sample. It was concluded therefore that its use would continue with both the rubber base and the chipseal wearing course.

## 3.5 Geogrid stabilised samples

Two different geogrids were tested, a large aperture (approx 60mm) tri-axial grid and a square (approx 40mm) grid, but time and resources dictated that the square grid could be tested in only one sample. Three different locations of the tri-axial geogrid were trialled: at the basecourse/'sub-base' interface (ie separated from the base by one layer of aggregate in order that the particles would be able to interlock with the geogrid, approximately 40–50mm above the base); at basecourse mid-height (ie approximately 150mm below the top surface); and at basecourse ¾ height (ie approximately 75mm below the top surface).

### 3.5.1 Sample 4 – geogrid at base

The first of the geogrid stabilised samples was prepared with the tri-axial geogrid. A section of geogrid was cut so as to fit into the ORAPT sample tray without any folding. The base of the ORAPT sample was covered with aggregate approximately one layer thick (40–50mm deep). The geogrid was then laid out on the sample and the remainder of the aggregate was added and spread over the geogrid (figure 3.21), totalling 2.05T and compacted as for previous samples. Compaction appeared to be neither easier nor more difficult than with samples with no geogrid (figure 3.22). Density and compaction data is given in table 3.4.

**Table 3.4 Density and moisture content calculations from NDM measurements: sample 4**

| Spot | WD ± 50 | DD ± 50 | % M ± 0.2% | % Comp ± 2 |
|---|---|---|---|---|
| 1 | 2323 | 2228 | 4.1 | 95 |
| 2 | 2342 | 2253 | 3.8 | 96 |
| 3 | 2340 | 2239 | 4.3 | 96 |
| 4 | 2339 | 2243 | 4.1 | 96 |
| 5 | 2365 | 2270 | 4.0 | 97 |
| 6 | 2320 | 2223 | 4.2 | 95 |

**Figure 3.21 Sample 4, placing and covering of tri- axial geogrid**

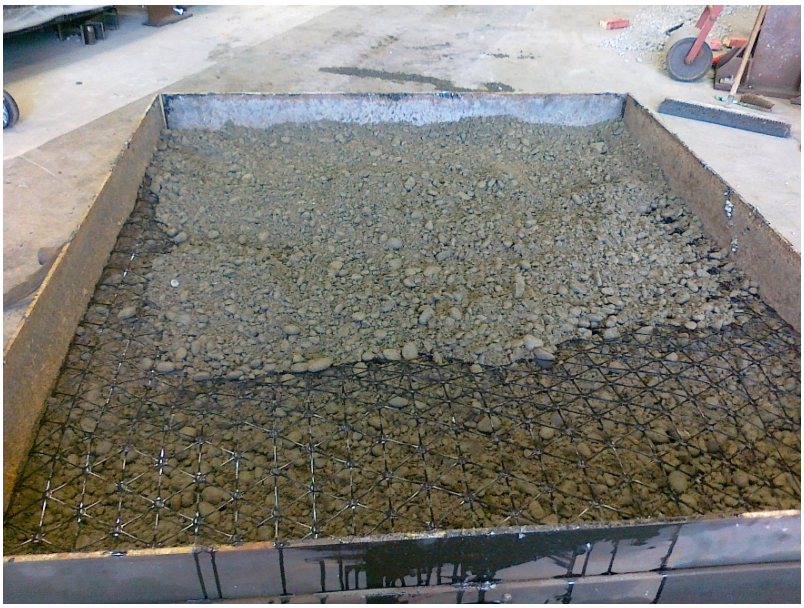

**Figure 3.22 Sample 4, compacted**

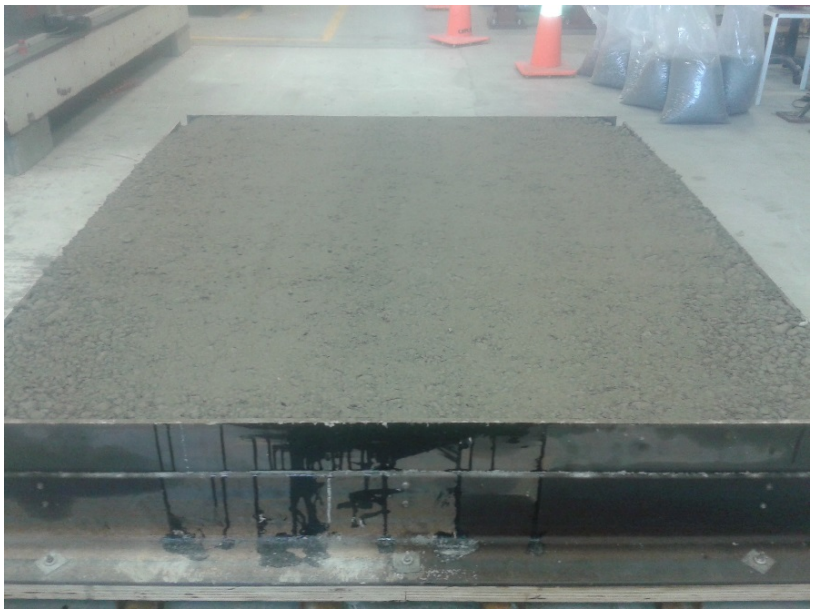

The sample was then covered with a grade 3/5 emulsion chipseal in exactly the same manner as sample 3. The chipseal was allowed to 'cure' for several days prior to wheel tracking.

Initial observations of wheel tracking of this sample showed chip roll-over and surface embedment into the surface of the basecourse, which appeared to initiate a rut beneath the wheel. However, measurement of the rut depth with increased tracking showed the final rut depth was approximately 37% that of the unstabilised sample 3 (figure 3.23). It was noted that the shapes and sizes of the shoulders formed were smaller than those formed in the unstabilised samples, but that they still did occur. The shape of the rut formation curve suggests rut formation had reached a maximum or had reached a steady state and would continue more slowly (figure 3.24).

**Figure 3.23 Rate of rut formation of tri- axial geogrid stabilised sample, geogrid at base of sample**

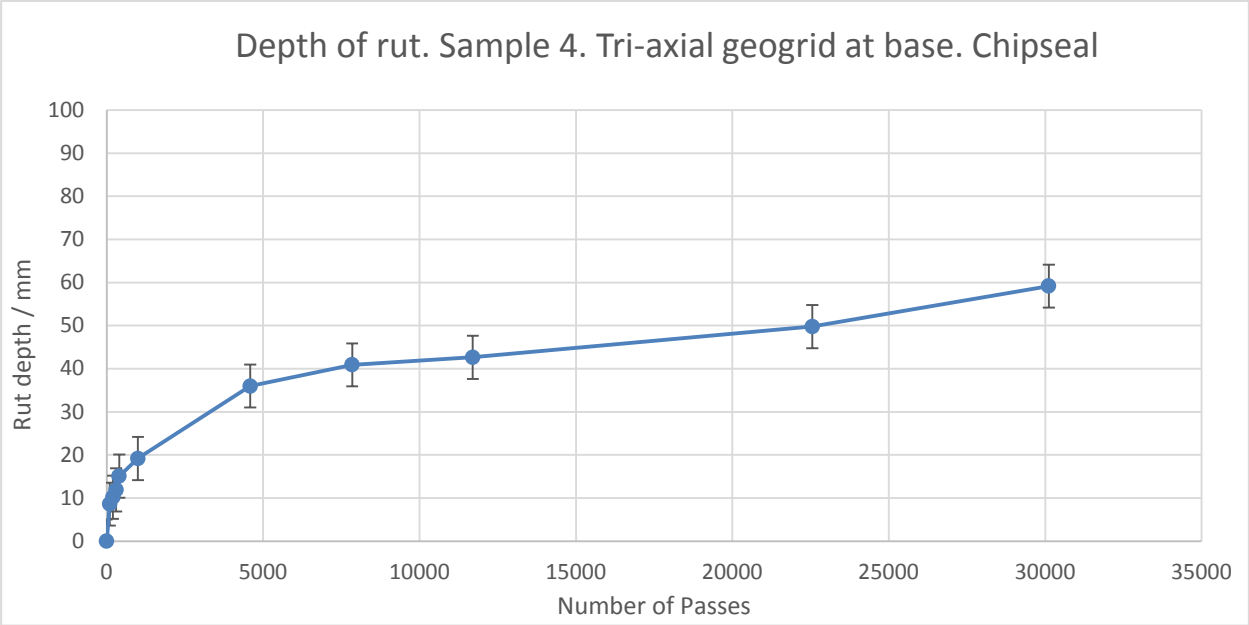


**Figure 3.24 Sample 4 after 30,000 passes**

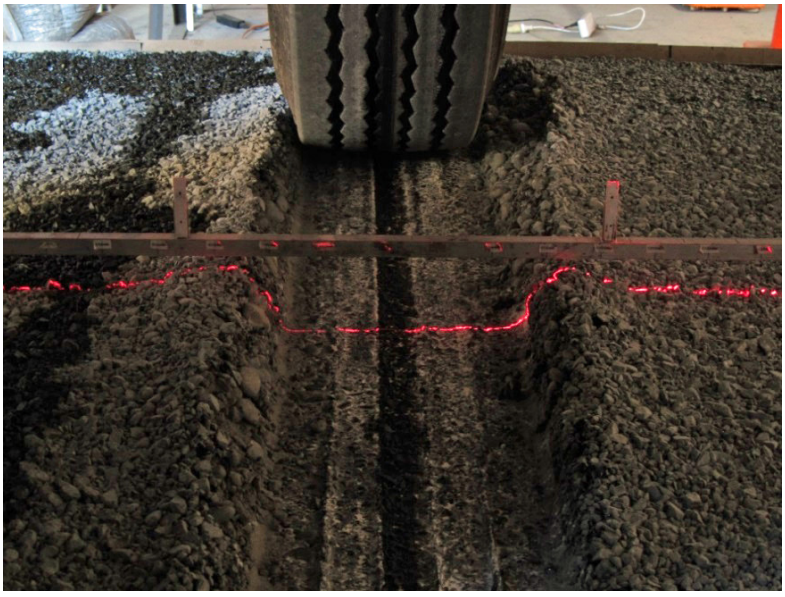

Visual examination of the basecourse in the rut following termination of the experiment suggested that

there was compaction of the material beneath the wheel path. There was little obvious suggestion, such as flow lines, that there was flow of aggregate away from the wheel path. The behaviour of the sample is considered further in chapter 4 where it is correlated with a FE model.

### 3.5.2 Sample 5 – geogrid at mid-height

The second geogrid stabilised sample was prepared with the tri-axial geogrid. A fresh sample was cut to fit into the ORAPT sample tray without any folding. The ORAPT sample tray was filled and levelled with aggregate to half height (140–150mm deep) but not compacted. The geogrid was then laid on the sample and the remainder of the aggregate (totalling 2.05T) was added, spread over the geogrid and compacted in the same manner as previous samples. Density, moisture and compaction data is given in table 3.5.

**Table 3.5 Density and moisture content calculations from NDM measurements: sample 5**

| Spot | WD ± 50 | DD ± 50 | % M ± 0.2% | % Comp ± 2 |
|---|---|---|---|---|
| 1 | 2323 | 2228 | 4.1 | 95 |
| 2 | 2342 | 2253 | 3.8 | 96 |
| 3 | 2340 | 2239 | 4.3 | 96 |
| 4 | 2339 | 2243 | 4.1 | 96 |
| 5 | 2365 | 2270 | 4.0 | 97 |
| 6 | 2320 | 2223 | 4.2 | 95 |

The sample was then covered with a grade 3/5 emulsion chipseal in exactly the same manner as samples 3 and 4. The chipseal was allowed to ‘cure’ for several days prior to wheel tracking. Wheel tracking at 20 kN tyre load was performed and the rate of rut formation was followed. Figures 3.25 to 3.29 show the rut and shoulder formation at different numbers of passes.

**Figure 3.25 Sample 5, rut formed after 200 passes at 20kN load**

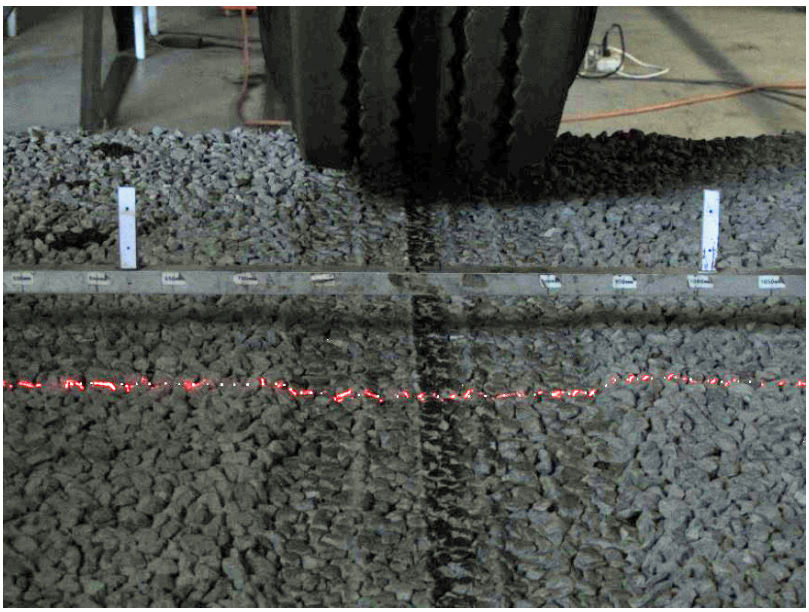

**Figure 3.26 Sample 5, rut formed after 7,200 passes at 20kN load**

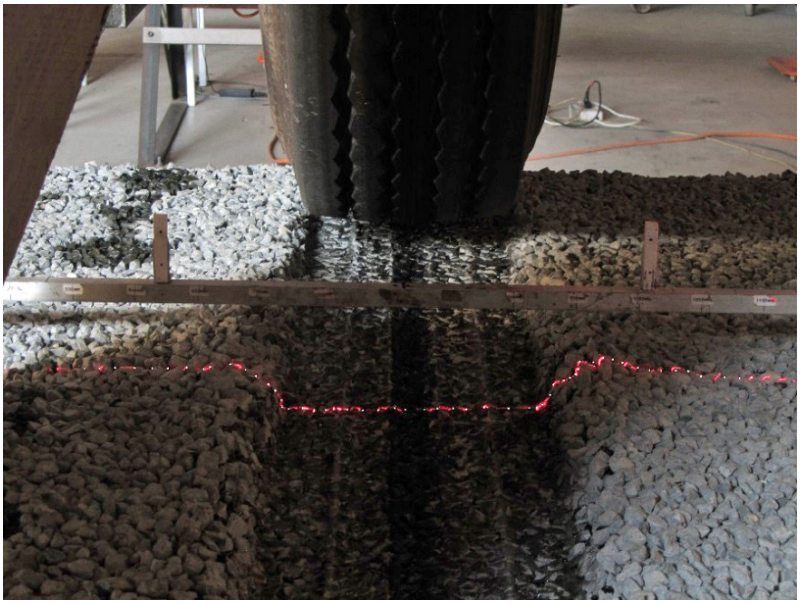

**Figure 3.27 Sample 5, rut formed after 30,100 passes at 20kN load**

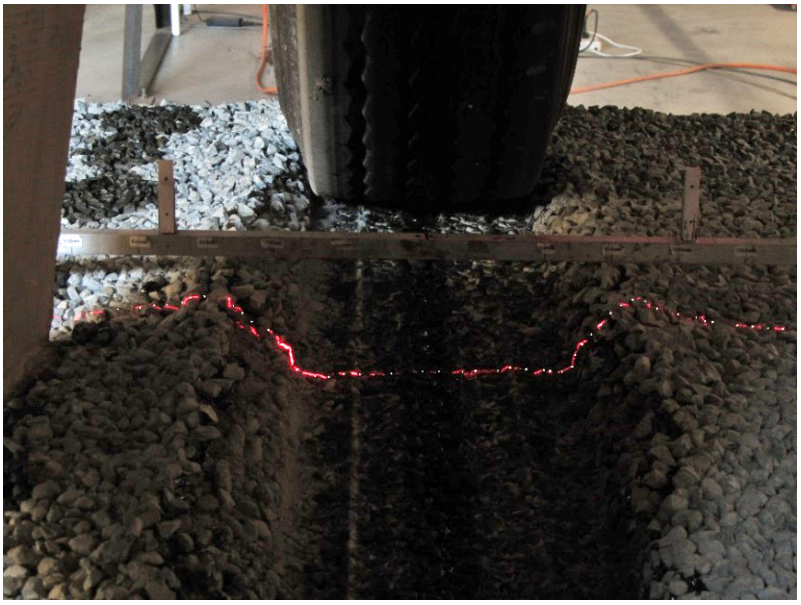

As for the earlier samples, we believe the rut shoulder is at least in part due to action of the sidewall of the tyre pushing and pulling on the basecourse material. It is likely there is some mass transfer, but we suggest that a significant proportion of the rut is due to additional compaction of the sample, rather than mass flow away from the rut. In this sample, the shoulders do not extend very far past the immediate wall of the rut. It might therefore be possible that the shoulders seen here are indeed due to action of the tyre on the walls of the rut, rather than mass transfer.

**Figure 3.28 Sample 5 view along rut after 30,100 passes at 20kN. Image shows chipseal surface and shouldering of the rut which may or may not be due to mass transfer**

**Figure 3.29 Sample 5, side view of rut and shoulder after 30,100 passes**

The rate of rut formation is followed in figure 3.30. The graph suggests the final rut depth for this stabilised sample, where the grid is positioned in the middle of the sample depth, is very similar to that of sample 4 (with the grid at the base of the sample) at approximately 42% of that of the unstabilised sample 3. We note, however, that the rutting rate might appear to have accelerated after 17,000 passes and was perhaps moving into a different behaviour phase. Bearing in mind the error inherent in the measurement, the two values from samples 4 and 5 could be considered to be about the same.

**Figure 3.30 Rate of rut formation of geogrid stabilised sample, geogrid at sample mid- height, chipseal**

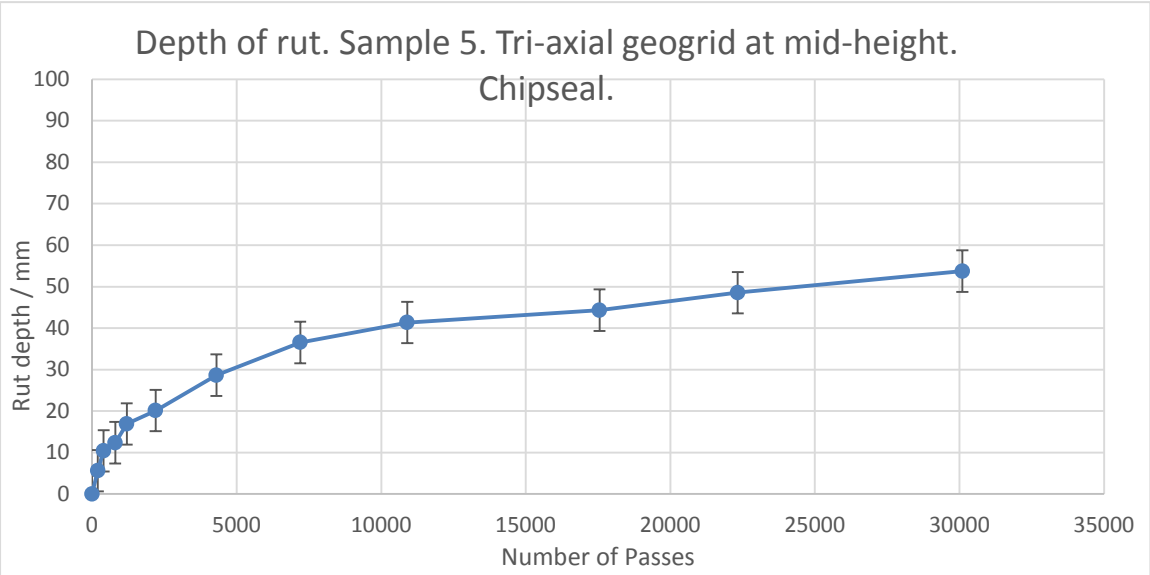


However, as was the case in earlier samples, the shouldering behaviour caused the wheel to be pushed off line and this experiment was terminated after 30,000 passes. There seems to be no advantage to placing the geogrid in the middle of the basecourse over placing it at the base of the sample. However, a word of caution might be raised in that there are different ways in which to install the grid, such as compacting up to the level of geogrid installation, then compacting the remainder of the sample (ie multiple lifts). In this work, samples were compacted in a single lift after all the aggregate was installed; however, compaction in multiple lifts might produce an improved result as indicated in the RLT test results (section 3.1).

Figures 3.31 to 3.33 show the surface of sample 5 after removal of the chipseal. While it is difficult to calculate actual values, visual inspection of the rut and the surrounding edges/shoulders suggests the volume created in the rut would not be filled completely by the volume created in the parts of the shoulders that extend above the datum surface. This in turn suggests the rut is created by a combination of compaction and mass transfer. The behaviour of the sample is further considered in section 4 and correlated with a FE model.

**Figure 3.31 View of rut, along centreline, following removal of chipseal covering, showing compaction along wheel path and lift of shoulders**

**Figure 3.32 View of rut from left side, showing shape of left- side shoulder**

**Figure 3.33 View of rut from right side, showing shape of right- side shoulder**

### 3.5.3 Sample 6 – geogrid at ¾ height

The third geogrid stabilised sample was prepared with the tri-axial geogrid at approximately 75mm below the top surface. While this is unlikely to be done in service, observations of this system have been that damage occurs at the surface of the sample. This was demonstrated in sample 2, where it was possible to stabilise the surface of the sample with asphalt. Therefore one rationale was that if it is possible to restrict mass transfer at or near to the surface, ie shear and/or consolidation, then it might be possible to restrict the amount of rutting that occurs. Compaction of the sample was again performed in a single lift, and again it was observed that significant movement of the sample occurred as compaction began, but then that compaction proceeded normally.

As for the previous geogrid stabilised samples, this sample was surfaced with a bitumen emulsion grade 3/5 chipseal which was allowed to 'set' for several days prior to wheel tracking. The sample as prepared is shown in figure 3.34 and presents a surface that while not perfectly flat, was free from undulations that would affect the wheel tracking.

However, immediately upon applying the wheel load, the sample began to rut. The rate of rut formation was significantly faster than that observed in both samples 4 and 5, and indeed, faster than that observed in sample 1. After 1,500 passes a rut of approximately 65mm had already formed, along with significant shouldering (figure 3.35). The shoulders did not extend very far beyond the immediate vicinity of the rut below the wheel path (figure 3.36), but did rise sharply above the rut. It can also be seen in figure 3.35 (as it can in images of previous samples) that as the wheel path approached the walls of the sample container the depth of the rut decreased and the shoulders disappeared. This is additional evidence for containment effects produced by the sidewalls of the sample container. Tracking of this sample was terminated at 1,550 passes.

Following termination, the chipseal was removed from the sample and the sample examined. It was found that rather than being 75mm below the surface, in the wheel path/rut the geogrid was only 50mm below the surface (figure 3.37). It was clear that a proportion of the rut was due to embedment of the chip into the seal and also into the base below it. It was also found that the portion of the surface of the sample in the wheel path was not solid, in that it could be pushed a few millimetres up and down by hand. This

seems to indicate that the thin layer of basecourse above the geogrid was not sufficient to maintain the integrity of the sample. It is also, perhaps, an indicator that if a pavement were to be constructed with a geogrid in a position other than at the base, it would need to be constructed in multiple lifts, ie one lift to the geogrid position, the second above the geogrid. The behaviour of the sample is further addressed in section 4 where the behaviours and FE analyses are considered.

**Figure 3.34 Geogrid stabilised sample 6 prior to wheel tracking**

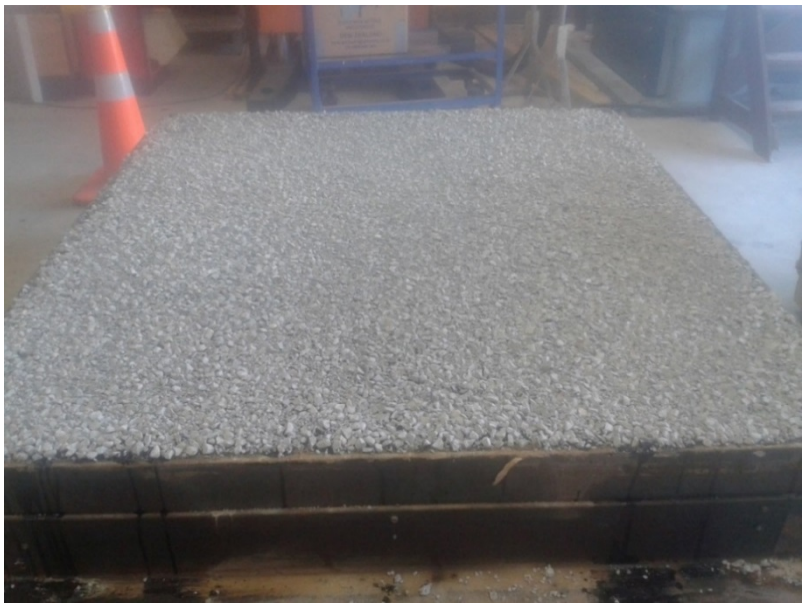

**Figure 3.35 View of rut after 1,550 passes showing shouldering on both sides of the deformation**

**Figure 3.36 Detailed view of shoulder on one side of rut showing short distance effect**

**Figure 3.37 Excavated sample showing reduced thickness above geogrid, 75mm to 50mm**

**Figure 3.38 Rate of rut formation of geogrid stabilised sample 6, geogrid at sample 3/4- height**

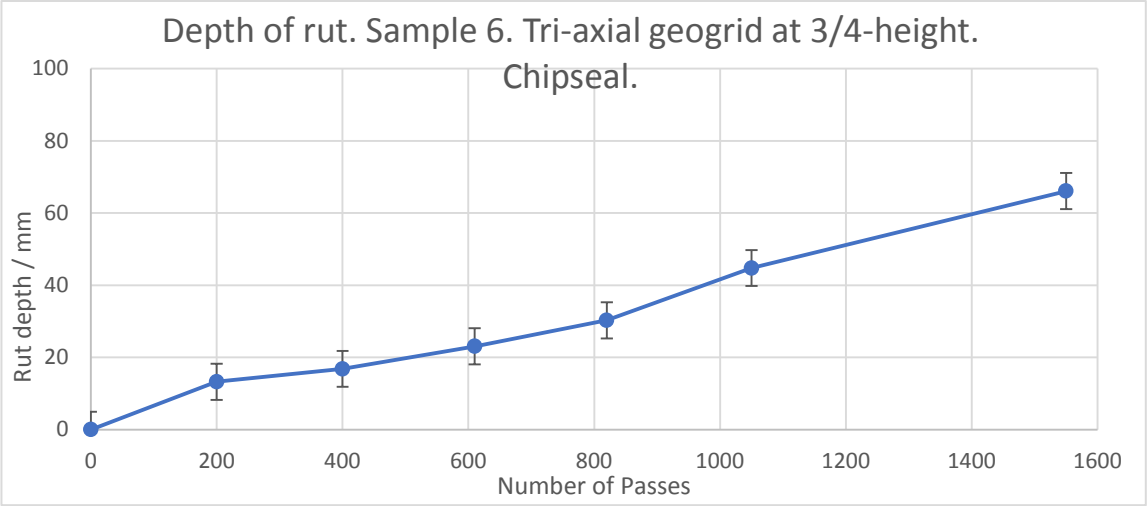


Figure 3.38 shows the graph of rate of rut formation for sample 6 and it seems clear that the rut formation was rapid and not going to slow until failure of some kind was established. Visual analysis of the material also did not suggest increased degree of compaction of the aggregate. This indicated that some of the rut was due to embedment of the chip, perhaps the first 10mm; the remainder was due to mass transfer away from the wheel path.

### 3.5.4 Sample 7 – square geogrid at sample base

The performance of the tri-axial geogrid with the grid placed at the base of the sample, was compared with that of a square-shaped geogrid or aperture approx. 40mm (see figure 2.2), also with the grid placed at the base of the sample. The ORAPT sample was prepared in the same manner as it was for all of the other samples, with the exception of the installation of the different geogrid sample. Sample 7 was compacted and surfaced with an emulsion 3/5 racked in chipseal in the same manner as samples 3 to 6 and then wheel tracked in the same fashion with a 20kN load being applied immediately. Density and moisture values were all comparable to the previous samples, as shown in table 3.6.

**Table 3.6 Density and moisture content calculations from NDM measurements: sample 7**

| Spot | WD ± 50 | DD ± 50 | %m ± 0.2% | % Comp ± 2 |
|---|---|---|---|---|
| 1 | 2,322 | 2,227 | 4.1 | 95.2 |
| 2 | 2,351 | 2,245 | 4.5 | 95.9 |
| 3 | 2,306 | 2,221 | 3.7 | 94.9 |
| 4 | 2,371 | 2,271 | 4.2 | 97.1 |
| 5 | 2,368 | 2,269 | 4.2 | 95.2 |
| 6 | 2,336 | 2,233 | 4.4 | 95.4 |

Visual observations suggested a difference in the behaviour of this sample over those using the first geogrid type where the deformation of the sample surface appeared to occur at a reduced rate. Indeed, as can be seen in figure 3.39, the rate of rut formation with increasing number of wheel passes was lower than that of the previous samples. After an equivalent 30,000 wheel passes (to sample 4) the sample presented a final rut depth that was reduced by approximately 60% over the unstabilised sample 3.

**Figure 3.39 Rate of rut formation of square geogrid stabilised sample 7, with grid at base of sample**

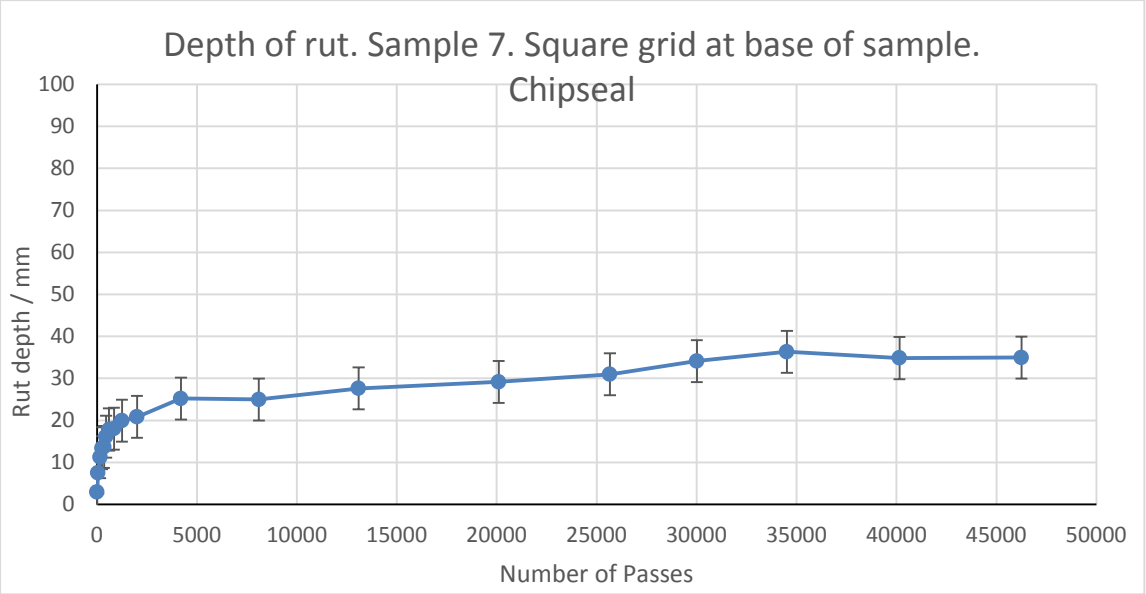


The graph in figure 3.39 suggests that the rut formation appears to have reached a maximum, or has slowed to a very low rate from perhaps 5,000 passes. Indeed, observation of the sample suggested that much of the apparent rut depth being measured from around 10,000 passes onwards was due to the growth of the sharp 'shoulder' on only one side of the sample (figure 3.40). It is thought that this 'shoulder' is due more to pick up or pushing of the side of the rut by the sidewall of the tyre rather than mass transfer from within the sample. The form of the 'shoulder' is sharper and smaller than previous samples and appears not suggestive of mass transfer (ie shoving). The graph shows the otherwise typical behaviour where the rate of rut formation at very early stages, up to approximately 5,000 passes, is significantly more rapid than the latter stages. This further reinforces the notion of shakedown occurring early in the experiment and may be a result of post-compaction densification beneath the wheel load.

**Figure 3.40 View of rut after 46,000 passes showing pick up only on left side of rut and relatively shallow rut**

### 3.5.5 Rut depth comparison – large aperture tri-axial and square geogrids

Figure 3.41 shows the comparison between the rates of rut formation of the 60mm aperture tri-axial and the 40mm square geogrid with each placed at the base of the sample (ie at the sub-base/basecourse interface). The graph suggests that the rate of rut formation for the two types of geogrid is very much the same early in the sample life, ie up to approximately 1,000 wheel passes. Beyond approximately 2,000 wheel passes, however, the rate of rut formation in the tri-axial sample appears to accelerate over that of the sample containing the square geogrid. It should be borne in mind that much of the measured rut in the sample containing the tri-axial geogrid was due to the tall shoulders that were formed as the basecourse was shoved upwards (figure 3.24).

**Figure 3.41 Comparison of rut formation rates between tri- axial and square geogrids at base of sample**

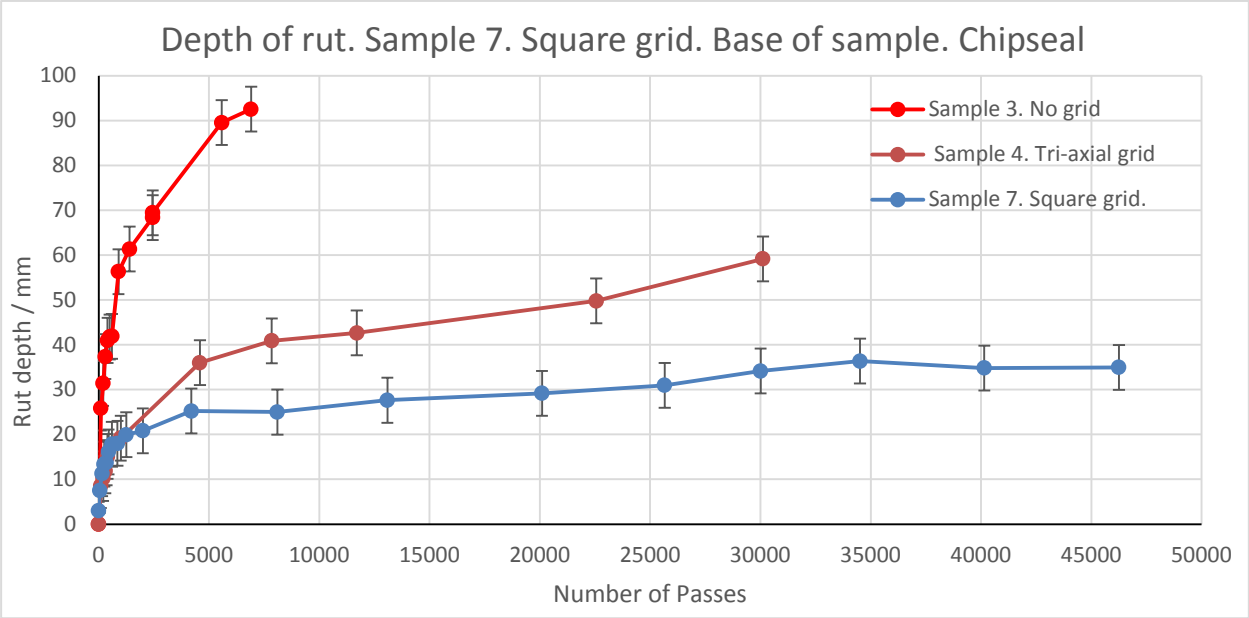


## 3.6 Geocell stabilised samples

Originally, the effects of geocells on the stability of the River Run aggregate were planned to be part of the study; however, the Steering Group decided this would not be necessary. The general efficacy of geocells is well established, but their installation costs are much higher than those of geogrids. It is reasonable to assume therefore that their use in New Zealand pavement construction will not be widespread.

# 4 Finite element analysis

The aggregate/geogrid system was analysed using a FE model developed at Opus Research (figure 4.1). The objective of the analysis was to evaluate the effectiveness of geogrids at different positions within the basecourse, and basecourses of different thicknesses. The outcome of the analysis would be measured in terms of stress and strain values within the basecourse and potential for lateral mass transfer (shear). Two different geogrid types (tri-axial and square) were modelled, but in the interests of comparison, only the tri-axial grid is discussed further here. Two different thicknesses of basecourse were investigated, with different base types (ie rigid or standard sub-base) but in the interests of comparison with our experimental system only the 150mm thick sample on a standard sub-base will be discussed further. The effect of the geogrid was modelled in six different positions away from the base of the sample, and in the interests of comparison with our experimental system only the placement of geogrids at 25mm (approximately ¾ height), 75mm (approximately mid height) and 125mm (approximately the base) below the basecourse surface will be discussed. Direction of travel of the load would be in the X direction, but in this case the load is stationary.

**Figure 4.1 The basic model geometry used in the analysis (a). A ¼ model was used due to the inherent symmetry and to ease computing time. In the case presented here, the model sits on a standard sub- base (b)**

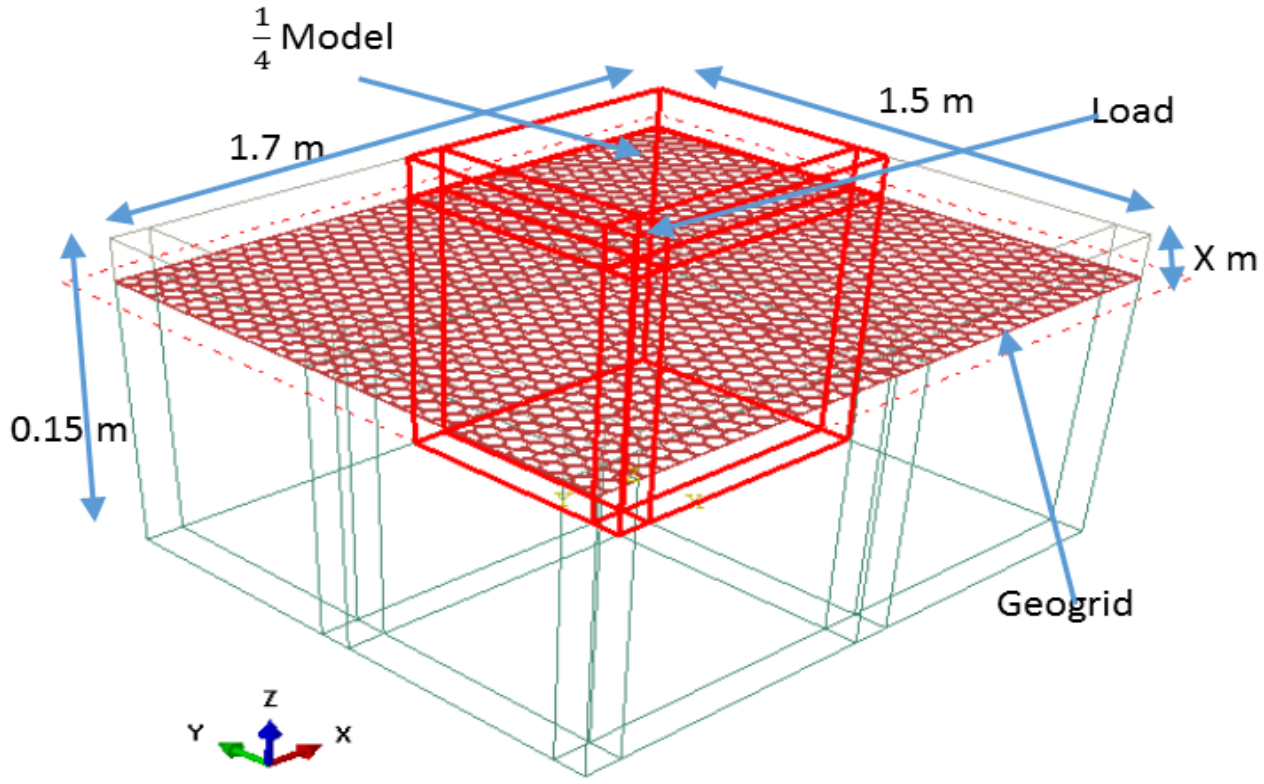


(a)

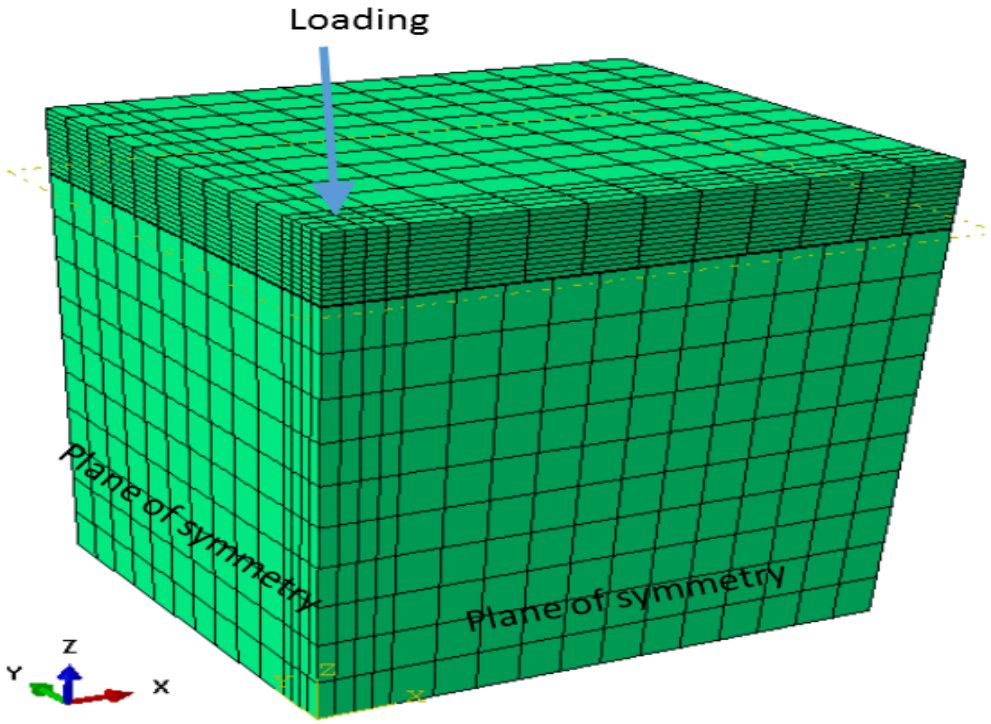


(b)

The general purpose FE program ABAQUS was used in this investigation to simulate the deformation process as shown in figure 4.1(b). By making use of symmetry in the geometry only one quarter of the model was considered. The boundary conditions of the model surfaces were adapted to create a quarter-model. The boundary conditions were set to 'pinned' ($U_1=UR_2=UR_3=0$) in the bottom, X-symmetry ($U_1=U_2=U_3=0$) and Y-symmetry ($U_2=UR_1=UR_3=0$) (in figure 4.1(b)). Here the displacements and rotations are $U_i$ and $UR_i$ respectively, and i=1,2,3 correspond to X, Y, Z axis.

The FE model contains granular basecourse material and geogrid. The resilient behaviour of granular materials is influenced by stress level, density, grain size, aggregate type, particle shape, moisture content and the number of load applications. There are several mathematical models that have been developed using different stress components. One of the most popular models was developed using RLT testing by Uzan (Uzan 1992; Werkmeister et al 2005):

$$E_1 = k_1 p_a \left(\frac{\theta}{p_a}\right)^{k_2} \left(\frac{\tau_{oct}}{p_a} + 1\right)^{k_3} \quad (4.1)$$ (Equation 4.1)

Where

$$\theta = \frac{\sigma_1+\sigma_2+\sigma_3}{3}$$

$$\tau_{oct} = \frac{\sqrt{(\sigma_1-\sigma_2)^2+(\sigma_2-\sigma_3)^2+(\sigma_3-\sigma_1)^2}}{3}$$

$$p_a = 100 \text{ kPa}$$

$E_1$, is resilient modulus, $k_1$, $k_2$, $k_3$ are constants, $\sigma_1$, $\sigma_2$ and $\sigma_3$ are principal stresses. An isotropic model has the same modulus in all directions, while an anisotropic model has different material properties in the horizontal

and vertical directions, and it is defined by $n=E_1/E_3$. Here $E_3$ is the modulus normal to the plane of isotropy.

The material model described above was implemented in ABAQUS using user-written subroutine UMAT, but several materials parameters $k_1$, $k_2$, $k_3$ and n are unknown. In order to improve upon RLT tests for the constants, laboratory and field experiments (falling weight deflection/strain gauges) were conducted to estimate the constants appearing in the material model using the inverse modelling technique (Kathirgamanathan and Herrington 2014). The resulting estimated values of constants are listed in table 4.1.

**Table 4.1 Optimised values of constants**

| n | $k_1$ | $K_2$ | $K_3$ |
|---|---|---|---|
| 0.15 | 6,600 | 1.5 | -0.4 |

A linear elastic material model was used for the geogrid and the manufacturer's material parameter values were used (E=860MPa, v=0.25). The interface between geo-grid and granular material was modelled using two different traditional contact interaction features: (a) perfect adhesion of the basecourse to the geogrid structure (the perfectly rough, no-slip, or bonded interface condition), and (b) zero adhesion (the full slip or smooth interface condition) available within the ABAQUS environment. The load applied to the model attempted to mimic that found in the experimental in that it was longitudinal and asymmetric. It was anticipated, however, that this would introduce some error into the outcome of the analysis. The shape and magnitudes of the loads applied by the Austroads standard tyre had been previously determined (figure 4.2). The load used in the model was therefore not a point load but rather a distributed load that more accurately represented the actual load applied by the Austroads truck tyre.

**Figure 4.2 Distribution of loads applied to the sample. In considering the ¼ model, only ¼ of the load is was considered**

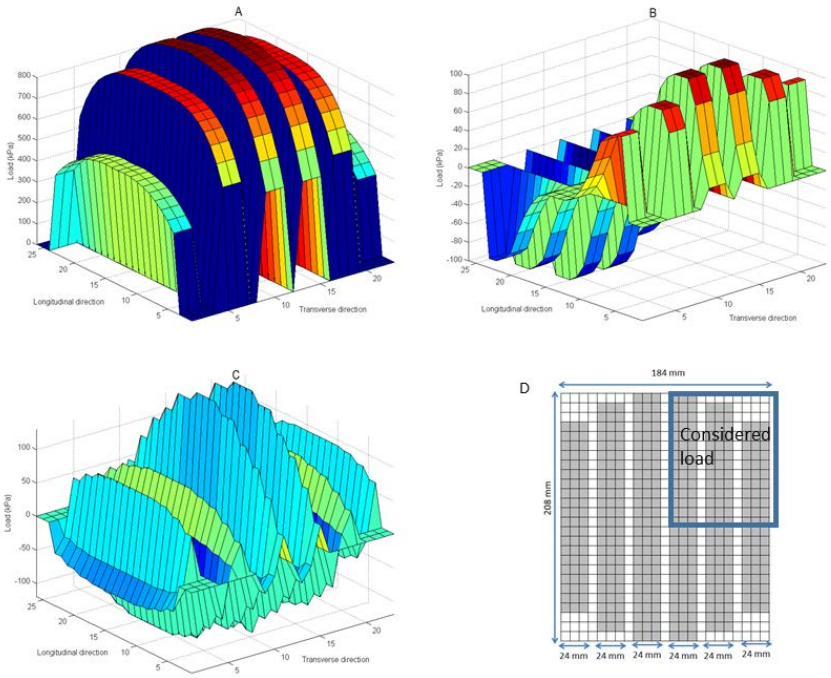


Figure 4.3 shows the contour plot of vertical displacement under a truck tyre load. The upper section and the lower sections represent the granular material and the geogrid at the interface can be seen, as well as the corner representing the applied load.

**Figure 4.3 Finite element model of pavement- deformed basecourse, geogrid, sub- base**

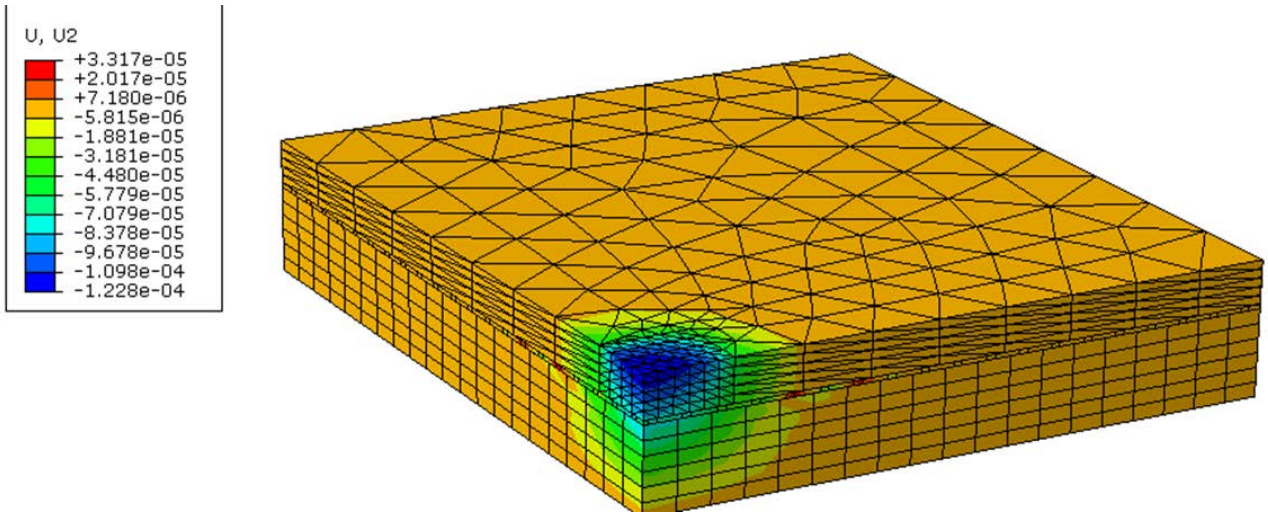


The transverse movement of material was modelled in the Z direction of the YZ plane (Y is the vertical axis). The model with no geogrid installed displays significant displacement potential throughout the sample, with maximum stress at the surface and in the interior of the model. Conversely, the sample with geogrid near the surface displays the greatest potential for transverse stress distribution.

**Figure 4.4 Transverse movement (z direction – yz plane) and associated stress values**

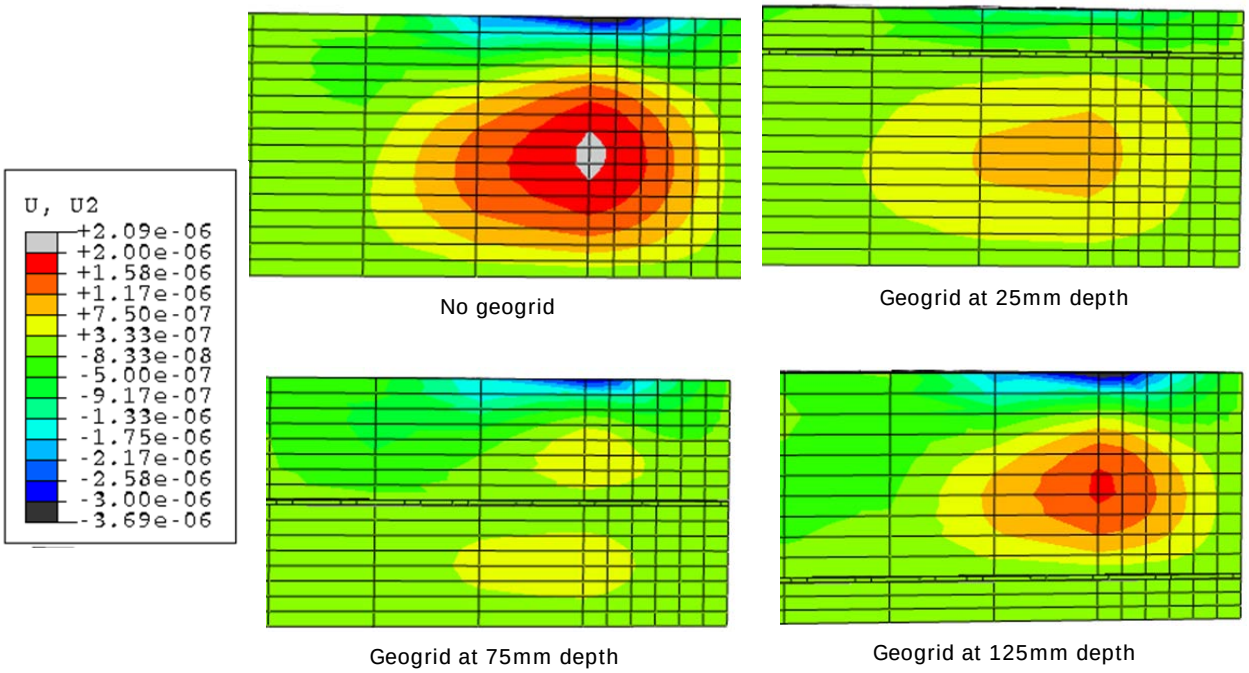


Using the same model, the vertical stress distribution was calculated. This would demonstrate the effect the geogrid placement would have on dispersing vertical load applied to the basecourse.

**Figure 4.5 Vertical stress distribution with geogrid at different positions in basecourse; minimum observed stress shown as green**

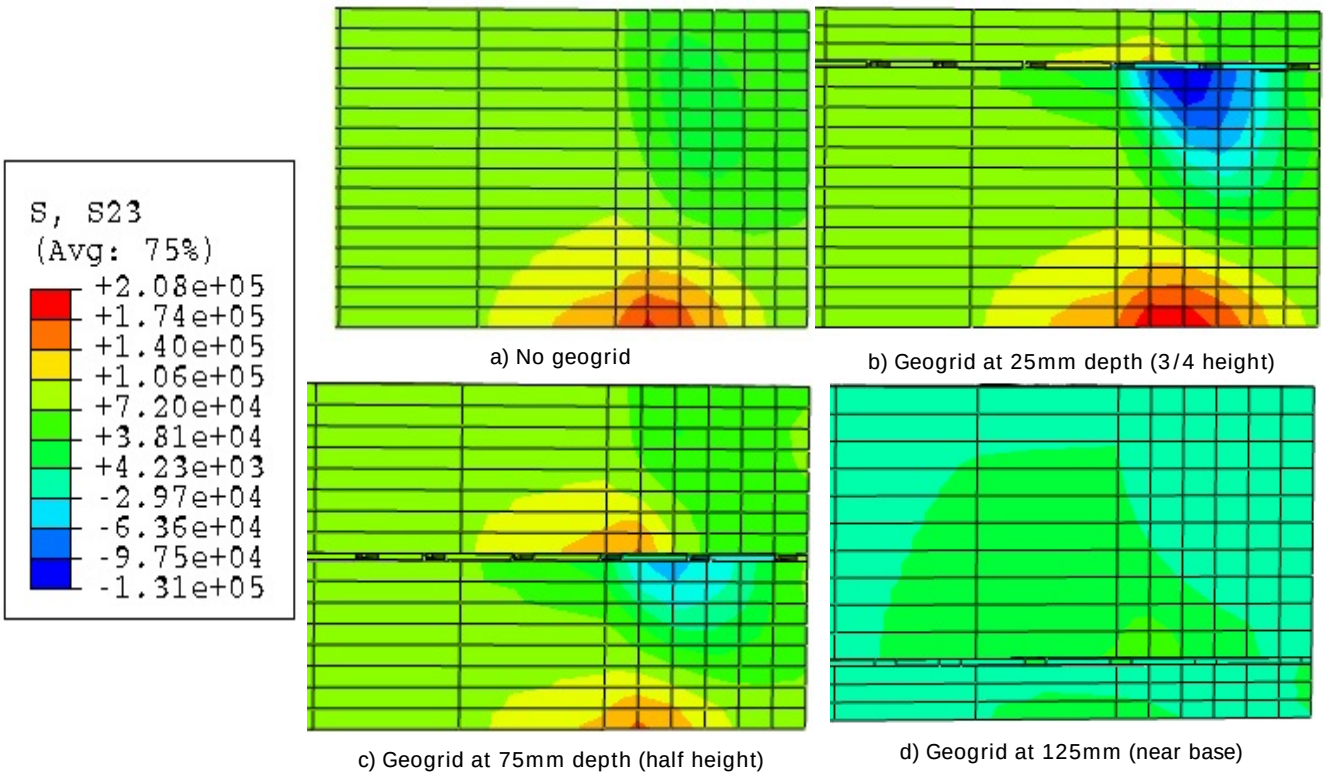


a) No geogrid

b) Geogrid at 25mm depth (3/4 height)

c) Geogrid at 75mm depth (half height)

d) Geogrid at 125mm (near base)

Figure 4.5 suggests that placement of the geogrid at or near the base of the basecourse sample has the greatest potential for vertical stress distribution throughout the sample.

The conclusions reached from our very preliminary FE analysis of this system were in line with those of previous studies as detailed above, that placement of the geogrid at the base of the basecourse layer produces the greatest benefit with regard to stress distribution and ultimately to reduction in permanent deformation.

# 5 Conclusions and recommendations

## 5.1 Conclusions

This research project set out to examine the ability of geogrid products to 'reinforce' basecourse aggregate materials under shear or aggregates of compromised geology. Analysis of the literature indicated that the concept of stabilisation, rather than reinforcement, should be considered when applying geogrids in pavements. During establishment of the terms of the project, it was decided to focus on the application of the geogrid technologies in concert with a low-cost, but abundant, river gravel aggregate from the Canterbury region. This material consists of greywacke gravels originating from the Southern Alps, carried down rivers to the Canterbury Plains area. As such they are weathered and very tough, but at the same time they are round with almost no flat faces and contain significant amounts of river sand (also round), but small amounts of intermediate-sized particles. Current understanding is that such aggregate materials would be poorly suited as basecourse aggregates and would readily shear or flow under load conditions. However, asset managers and contractors in the region are currently using this material, designated here as River Run aggregate, to prepare bases for pavements due to its low cost and ready availability.

As the project proceeded it became clear that only one specimen of each variable could be tested. More set-up and unstabilised samples were required in order to establish the experimental conditions than were anticipated and some equipment difficulties were also experienced, thereby impinging on the time and budget available for the project. Anecdotal information from contractors and consultants suggests that rut-depth differences between roads and field test specimens of ±30% can be common, and experience with earlier work with the more controlled ORAPT experiment has indicated that rut-depth differences between repeat specimens of approximately ±10% can be expected. However, due to the lack of statistically relevant numbers of repeat samples in this work, the error expressed in each result can only be that inherent in the measurement of each point, which was estimated at ±5 mm.

The results obtained here in the ORAPT experiment indicate it is possible to prepare a compacted basecourse using the supplied aggregate. Initial compaction is difficult with significant movement of the aggregate, but once a degree of compaction is initiated, further compaction proceeds to the maximum compaction indicated by the supplier.

The surface of the compacted sample possesses virtually no particle interlock and therefore virtually no inherent strength. Therefore, tyre-induced shear of the first few layers of aggregate in the surface of the sample occurs readily. However, the surface of the sample can be stabilised with a chipseal or even more effectively with an asphalt wearing course layer. The latter in particular locks up the surface layers providing a strong degree of strength and resistance to compaction and shearing of the basecourse and to subsequent rutting.

The ORAPT experiment suggested that stabilisation of the River Run basecourse with geogrid might reduce the final rut depth by between 40% and 60%. The smaller aperture grid produced shallower rut depth indicating that aperture matching to the aggregate is very important. Only small differences between the rate of rut formation with geogrid stabilisation at the base of the sample, or at mid-height of the sample were found. The rate of rut formation with geogrid stabilisation near the surface of the sample however, was observed to be much faster than with the grid at lower placements. While this could be a result of the sample preparation method (ie one lift as opposed to two), this result does mirror that of other studies, which have shown that maximum benefits of geogrid installation come with the grid at or near to the sub-base/basecourse interface.

The results from the ORAPT sample testing can be compared favourably with those obtained from RLT testing where reduction in shear of the River Run aggregate of approximately 50% was found with the large aperture geogrid stabilisation. The same experiment with smaller aperture grid was unfortunately not conducted in this case. One difference between the RLT test and the ORAPT experiment that should be tested was that the ORAPT samples were compacted in a single lift, rather than multiple lifts. This may possibly mean the densities of the ORAPT samples were not as high as might otherwise have been achieved, possibly leading to in-service compaction and at least some of the rutting caused by in service consolidation. The increase in sample modulus was less than that value and therefore suggested that bulk modulus on its own was not a sufficient value for characterising a geogrid-stabilised aggregate sample. It is clear that geogrids can offer significant stabilisation of the River Run aggregate material.

## 5.2 Recommendations

From the results obtained in this work, the following recommendations can be made:

- It may be possible that the tri-axial geogrid selected was inappropriate for the particle size distribution of the aggregate used. Selection of a different sized tri-axial geogrid may improve the rutting performance of the tri-axial geogrid with this particular aggregate. The results obtained here indicate that close attention should be paid to appropriate sizing of geogrids with respect to the aggregate being used. Further investigations are recommended to test the applicability of a smaller aperture tri-axial geogrid.
- Stabilisation might be improved with geogrid placement at mid-height of the basecourse if the basecourse is prepared in two lifts.
- Stabilisation of the surface of this aggregate material with an asphalt concrete layer provides significant stabilisation and resistance to permanent deformation. This would be further improved over our test with a high-quality stone matrix asphalt or asphalt concrete surfacing.
- Combination of asphalt concrete or stone matrix asphalt surface, compaction in at least two lifts and installation of geogrid at either the sub-base/basecourse interface or the inter-lift interface is recommended.
- Geocells were not included in this study and it is recommended that at least one geocell variable should be examined.
- It is likely that aggregate stabilisation with cement or bitumen will provide further improved basecourse stabilisation especially in the problematic surface region of the basecourse. The combination of geogrids and binder should be investigated.
- Additional ORAPT samples should be examined to establish the repeatability of these results.
- Future ORAPT samples should be prepared in multiple (at least two) compaction lifts.

# 6 References

Abdel-Jawad, YA and WS Abdullah (2002) Design of maximum density aggregate grading. *Construction and Building Materials 16*: 495–508.

Abu-Farsakh, MY, J Gu, GZ Voyiadjis and Q Chen (2014) Mechanistic-empirical analysis of the results of finite element analysis on flexible pavement with geogrid base reinforcement. *International Journal of Pavement Engineering 15*, no.9.

Al-Qadi, IL, SH Dessouky, J Kwon and E Tutumluer (2012) Geogrid-reinforced low-volume flexible pavements: pavement response and geogrid optimal location. *Journal of Transportation Engineering 138*, no.9: 1083–1090.

Archer, S (2008) *Subgrade improvement for paved and unpaved surfaces using geogrids*. Professional Development Series, Contech Engineered Solutions.

AASHTO (2005) *Practice PP 46-01. Recommended practice for geosynthetic reinforcement of the aggregate base course of flexible pavement structures*.

Berg, RR, BR Christopher and SW Perkins (2000) Geosynthetic reinforcement of the aggregate base course of flexible pavement structures. *GMA white paper II. Geosynthetic Materials Association*, Roseville, MN. 176pp.

Bhandari, A, J Han and RL Parsons (2014) Two-dimensional DEM analysis of behavior of geogrid-reinforced uniform granular bases under a vertical cyclic load. *Acta Geotechnica: 1–12*.

Brink, A-C, E Horak and A Visser (2004) *Improvement of aggregate interlock equation used in mechanistic design software.*

British Standards Institution (2004) BS EN 13286-7:2004 Unbound and hydraulically bound mixtures. Cyclic load triaxial test for unbound mixture.

Cavanaugh, J and J Kwon (2008) Developing mechanistic-empirical design methods. *Civil and Structural Engineer*. Accessed 23 August 2015. http://cenews.com/article/6096/developing-mechanistic-empirical-design-methods October.

Chaddock, BCJ (1988) Deformation of road foundations with geogrid reinforcement. *Transport and Road Research Laboratory report 140*.

Chrismer, S (1997) Test of Geoweb to improve track stability over soft subgrade. *Report TD 97-045*, Technology Department, Association of American Railroads, Washington DC.

Craig, RF (1997) *Soil mechanics.* 6th ed. London: E & FN Spon. 303pp.

Das, S and MR Choudhury (2015) A comparative study between traditional method and mix design with industrial bi-products for the testing and repairing of bituminous pavements. *World Journal of Civil Engineering and Construction Technology 2*, no.1: 042–050.

Dondi, G (1994) Three-dimensional finite element analysis of a reinforced paved road. In *Proceedings of the 5th International Conference of Geotextiles, GeoMembranes and Related Products 1*: 95–100.

Drucker, DC and W Prager (1952) Soil mechanics and plastic analysis for limit design. *Quarterly of Applied Mathematics 10*, no.2: 157–165.

Giroud, JP (1984) Geotextiles and geomembranes. *Geotextiles and Geomembranes 1*, no.1: 5–40.

Giroud, JP and J Han (2004) Design method for geogrid-reinforced unpaved roads, Part I theoretical development. *ASCE Journal of Geotechnical and Geoenvironmental Engineering 130*, no.8: 776–778.

Giroud, JP and L Noiray (1981) Geotextile-reinforced unpaved road design. *Journal of the Geotechnical Engineering Division*, ASCE 107, GT 9: 1233–1254.

Han, J, B Leschinsky, RL Parsons, A Rosen and J Yuu (2008) Technical review of geocell-reinforced basecourses over weak subgrade. In *Proceedings of 1st Pan-American Conference and Exhibition*, Cancun, Mexico. Vol. 1.1: 1022-1030.

Han, J, JK Thakur, RL Parsons, SK Pokharel, D Leshchinsky and X Yang (2013) A summary of research on geocell-reinforced base courses. In *Proceedings of International Symposium on Design and Practice of Geosynthetic Soil Structures*. Bologna, Italy. 14–16 October 2013. 351.

Howard, I and K Warren (2006) Finite element modelling approach for flexible pavements with geosynthetics. In *Proceedings of GeoCongress*, Atlanta, Georgia, 26 February – 1 March 2006: 1–6.

Huang, YH (2004) *Pavement analysis and design.* 2nd ed. Upper Saddle River, NJ: Pearson Prentice Hall.

Hudson, KC and GRW East (1991) Geotextiles. *Transit New Zealand research report 6*.

Jones, RH and AR Dawson (Eds) (1989) *Unbound aggregates in roads*. London: Butterworths.

Kathirgamanathan, P and PR Herrington (2014) *Numerical modelling of road with chipseal surfacing layer*. JUICE Accelerated Regional Development.

Kief, O, Y Schary and SK Pokharel (2014) High-modulus geocells for sustainable highway infrastructure. *Indian Geotechnical Journal, 14 September*.Koerner, RM (1998) *Designing with geosynthetics.* 4th ed. Upper Saddle River, NJ: Prentice-Hall.

Kwon, J and E Tutumluer (2009) Geogrid base reinforcement with aggregate interlock and modelling of associated stiffness enhancement in mechanistic pavement analysis. *Transportation Research Record: Journal of the Transportation Research Board 2116*: 85–95.

Kwon, J, E Tutumluer and M Kim (2005) Development of a mechanistic model for geosynthetic-reinforced flexible pavements. *Geosynthetics International 12*, no.6: 310–320.

Kwon, J, E Tutumluer and IL Al-Qadi (2009) Validated mechanistic model for geogrid base reinforced flexible pavements. *Journal of Transportation Engineering 135*, no.12: 195–926.

Kwon, J, E Tutumluer and H Konietzky (2008) Aggregate base residual stresses affecting geogrid reinforced flexible pavement response. *International Journal of Pavement Engineering 9*, no.4: 275–285.

Lay, MG (1990a) *Handbook of road technology.* Vol 1, 2nd ed. Melbourne: Gordon and Breach: 181–183.

Lay, MG (1990b) *Handbook of road technology.* Vol 1. 2nd ed., Melbourne: Gordon and Breach: 187–186.

Leshchinsky, B and H Ling (2013a) Effects of geocell confinement on strength and deformation behaviour of gravel. *Journal of Geotechnical and Geoenvironmental Engineering 139*, no.2: 340–352.

Leshchinsky, B and H Ling (2013b) Numerical modelling of behaviour of railway ballasted structure with geocell confinement. *Geotextiles & Geomembranes 36*, no.1: 33–43.

Moayedi, H, S Kazemian, A Prasad and BBK Huat (2009) Effect of geogrid reinforcement location in paved road improvement. Electronic Journal of Geotechnical Engineering, Bund. 14pp.

Netlon Industries (1984) *Netlon Industries technical report 1984*.

NZ Transport Agency (2005) *B2/02:2005 Specification for construction of unbound granular pavement layers*.

Patrick, J, P Kathirgamanathan, S Cook, P Herrington and H Arampamoorthy (2011) Small-scale accelerated pavement testing machine. *Road and Transport Research 20*, no.3: 33–39.

Perkins, SW (1999) Geosynthetic reinforcement of flexible pavements: laboratory based pavement test sections. *Report FHWA/MT-99/8106-1*. Montana Department of Transport.

Perkins, SW (2001) Mechanistic-empirical modelling and design model development of geosynthetic reinforced flexible pavements. *FHWA/MT-01-002/99160-1A*. Montana Department of Transport.

Perkins, SW, BR Christopher, EL Cuelho, GR Eiksund, CS Schwartz and G Svanø (2009) A mechanistic-empirical model for base-reinforced flexible pavements. *International Journal of Pavement Engineering 10*, no.2: 101–114.

Perkins, SW and MQ Edens (2002) Finite element and distress models for geosynthetic-reinforced pavements. *International Journal of Pavement Engineering 3*, no.4: 239–250.

Perkins, SW and MQ Edens (2003) A design model for geosynthetic-reinforced pavements. *International Journal of Pavement Engineering 4*: 37–50.

Perkins, SW and M Ismeik (1997) A synthesis and evaluation of geosynthetic-reinforced base layers in flexible pavements: Part II. *Geosynthetics International 4*, no.6: 605–621.

Pokharel, SK, J Han, C Manandhar, X Yang, B Leshchinsky, I Halahmi and RL Parsons (2011) Accelerated pavement testing of geocell-reinforced unpaved roads over weak subgrade. *Journal of the Transportation Research Board 2204*: 67–75.

Potter, JF and EWH Currer (1981) The effect of a fabric membrane on the structural behaviour of a granular road pavement. *Transport and Road Research Laboratory report LR 996*. Wokingham: TRL.

Roscoe, KH and JB Burland (1968) On the generalised stress-strain behaviour of 'wet' clay. Pp535–609 in J Heyman and FA Leckie (Eds) (1968) *English plasticity*, Cambridge University Press.

Ruddock, EC (1982) *Fabrics and meshes in roads and other pavements: a state of the art review*. London, CIRIA.

Ruddock, EC, JF Potter and AR McAvoy (1982) *A full scale experiment on granular and bituminous road pavements laid on fabrics*. In *Proceedings of the 2nd International Conference on Geotextiles*. IFAI, Vol. 2, Las Vegas, Nevada, August 1982, pp365–370.

Seward, J, R Williamson and J Mohney (1977) *Guidelines for the use of fabrics in construction and maintenance of low-volume roads*. Portland OR: USDA, Forest Service.

Shen, S and H Yu (2011) Characterize packing of aggregate particles for paving materials: particle size impact. *Construction and Building Materials 25*, no.3: 1362–1268.

Song, Y and PSK Ooi (2010) Interpretation of the shakedown limit from multistage permanent deformation tests. *Transport Research Record: Journal of the Transportation Research Board 2167*: 72–78.

Transit NZ, RCA and Roading NZ (2005) *Chipsealing in New Zealand*. Wellington: Transit New Zealand, Road Controlling Authorities, Roading New Zealand.

US Army Corps of Engineers (USACOE) (2003) *Use of geogrids in pavement construction*. WAhington DC: USACOE.

Uzan, J (1992) Resilient characterization of pavement materials. *International Journal for Numerical and Analytical Methods in Geomechanics 16*, no.6: 453–459.

van Blerk, G and C Fahey (2013) Pavement design and construction technique using high strength stone interlock cemented aggregate matrix. Pp395–410 in *Airfield and highway pavement 2013: sustainable and efficient pavements*. IL Al-Qadi and S Murrell (Eds). American Society of Engineers.

Webster, SL (1992) Geogrid reinforced base course for flexible pavements for light aircraft: test section construction, laboratory tests and design criteria. *US Army Corps of Engineers report DOT/FAA/RD-92-25*.

Werkmeister, S, AR Dawson and F Wellner (2005) Permanent deformation behaviour of granular materials and the shakedown concept. *Road Materials and Pavement Design 6*, no.1: 31–51.

Weston, B and T Edwards (2004) Investigation of conventional lime stabilisation of subgrades versus the use of geotextiles in road construction. In *Proceedings of the 2nd International Geotechnical & Pavements Engineering Conference*: 131–173.

Yang, X (2010) *Numerical analyses of geocell-reinforced granular solid under static and repeated loads*. PhD thesis, University of Kansas, Lawrence.

Yedeti, TF, B Birgisson, D Jelagin and A Guarin (2013) Packing theory-based framework to evaluate permanent deformation of unbound granular materials. *International Journal of Pavement Engineering 14*, no.3: 309–320.

Zhou, H and X Wen (2008) Model studies on geogrid- or geocell-reinforced sand cushion on soft soil. *Geotextiles & Geomembranes 26*, no.3: 231–238.